First-order coherent resonant tunneling through an interacting coupled-quantum-dot interferometer: Generic quantum rate equations and current noise

Bing Dong and X. L. Lei
Department of Physics, Shanghai Jiaotong University, 1954 Huashan Road, Shanghai 200030, China

Norman J. M. Horing
Department of Physics and Engineering Physics, Stevens Institute of Technology, Hoboken, New Jersey 07030, USA
(Received 18 December 2006; revised manuscript received 5 April 2007; published 13 February 2008)

We carry out a detailed analysis of coherent resonant tunneling through two coupled quantum dots (CQDs) in a parallel arrangement in the weak-tunneling limit. We establish a set of quantum rate equations in terms of the eigenstate representation by means of a generic quantum Langevin equation approach, which is valid for arbitrary bias voltage, temperature, and interdot hopping strength. Based on linear-response theory, we further derive the current and frequency-independent shot noise formulas. Our results reveal that a previously used formula for evaluating Schottky-type noise of a "classical" single-electron transistor is a direct result of linear-response theory, and it remains applicable for small quantum devices with internal coupling. Our numerical calculations show some interesting transport features (i) for a series CQD: the appearance of a negative differential conductance due to the bias-voltage-induced shifting of bare levels or a finite interdot Coulomb repulsion, and (ii) for a parallel CQD in strong interdot Coulomb repulsion regime: finite-bias-induced Aharonov-Bohm oscillations of current, and magnetic-flux-controllable negative differential conductance and a huge Fano factor.

DOI: 10.1103/PhysRevB.77.085309 PACS number(s): 72.10.Bg, 73.63.Kv, 73.23.Hk, 72.70.+m

I. INTRODUCTION

The investigation of quantum oscillations between two levels in a coupled-quantum-dot (CQD) system under transport conditions has been the subject of enormous interest over the past decade.[1,2] Recently, a CQD arranged in parallel between source and drain has been experimentally reported to constitute a mesoscopic quantum dot (QD) Aharonov-Bohm (AB) interferometer,[3–5] and it is believed that manipulation of each of the QDs separately and the application of magnetic flux piercing the device can provide controllable parameters for the design of transport properties by tuning quantum oscillations.[3–13]

To describe such quantum oscillations in quantum transport, master equations and a "quantum" version of rate equations were first proposed by Nazarov and co-workers,[14,15] and later derived from the Schrödinger equation,[16,17] respectively. These original works are mainly for a CQD in a series arrangement between leads in the limit of zero temperature and large bias voltage. The authors have generalized the quantum rate equations (QREs) for the case of a CQD interferometer in the same limit and employed them to study magnetic-flux-controlled photon-assisted tunneling.[13] Recently, a bias-voltage- and temperature-dependent generalization of the QREs was carried out by the authors, employing the nonequilibrium Green's function in the limit of weak dot-dot coupling.[18] However, the dot-dot coupling of the CQD device is usually tuned using gate voltage in experiments, and it may not be weaker than the tunnel coupling to external electrodes. Therefore, it is desirable to develop generic QREs without assuming weakness of the dot-dot coupling for the purpose of systematically analyzing the transport properties of a CQD system.

To accomplish this, we employ a generic quantum Langevin equation approach to derive the QREs in the eigenstate representation. The main result is the determination of a different coherent transfer term that emerges in all dynamic equations of the reduced density-matrix (RDM) elements stemming from the effective coupling between two eigenstates due to tunneling, which is absent from our previous results for QREs.[18] In addition, other coherent terms occur in the ensuing QREs for a CQD interferometer due to interference between the two path branches enclosing magnetic flux, which is responsible for the AB oscillation feature of transport, as expected.

In another emerging aspect of CQD systems, studies of current fluctuations have become an important topic.[19,20] Several analyses of shot noise in a CQD system have been undertaken by means of the QRE approach.[21–29] Most of these works have involved calculations in the large bias-voltage limit for CQDs in series[21–23,25,26] or in parallel.[29] Our earlier work was carried out with analyses based on our previous QREs and, correspondingly, it is only valid for the case of weak dot-dot hopping.[25] Moreover, some other recent studies of bias-voltage-dependent shot noise of a CQD have not treated the quantum coherence effect.[27,28] Therefore, in this paper, we will also analyze zero-frequency shot noise of an interacting CQD using the presently developed QREs, focusing our attention on the coherence and interference effects and its magnetic-flux dependence at both large and small bias voltages.

The outline of the paper is as follows. In Sec. II, we present our physical model for a CQD interferometer connected to two electrodes and derive a set of QREs using a generic quantum Langevin equation approach with a Markovian approximation in describing the dynamic evolution of the RDM elements under transport conditions. Such microscopically derived QREs are valid at arbitrary bias voltage and temperature, and dot-dot hopping strength as well. In this section, we also derive the current and frequency-independent shot noise formulas in terms of the RDM ele-

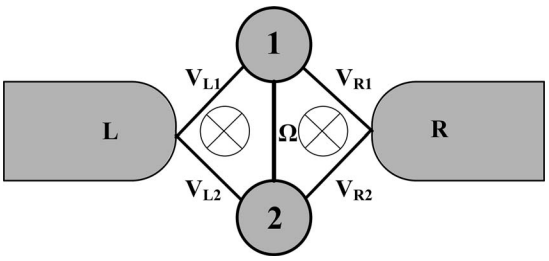

FIG. 1. Schematic diagram for coherent resonant tunneling through a parallel-coupled double quantum dot system in an Aharonov-Bohm interferometer.

ments using linear-response theory. Employing the obtained formulas, we then investigate the transport properties of a CQD in series in Sec. III, stressing the asymmetric transport property. Moreover, we study in detail the combined effect of the additional coherent transfer term and the two-pathway-interference term on current (Sec. IV) and on shot noise (Sec. V) of a CQD interferometer. A summary is given in Sec. VI.

II. HAMILTONIAN AND FORMULATION

The parallel-coupled interacting QD interferometer connected to two normal leads is illustrated in Fig. 1. The Hamiltonian is given by

$$H = H_L + H_R + H_D + H_T, \tag{1}$$

where H_η ($\eta = L$ and R) describes noninteracting electron baths in the left and right leads, respectively:

$$H_\eta = \sum_{\mathbf{k}} (\varepsilon_{\eta\mathbf{k}} - \mu_\eta) a^\dagger_{\eta\mathbf{k}} a_{\eta\mathbf{k}}, \tag{2}$$

with $a_{\eta\mathbf{k}}$ being the annihilation operator of an electron with momentum $\mathbf{k}$ and energy $\varepsilon_{\eta\mathbf{k}}$ in lead η, and μ_η being the effective Fermi energy of lead η. In our studies, a bias voltage V is taken to be applied symmetrically between the two electrodes, i.e., $\mu_L = -\mu_R = eV/2$, to sustain a persistent electron flow from one lead to the other. In equilibrium, $V=0$, we set $\mu_L = \mu_R = 0$. Throughout, we will use units with $\hbar = k_B = e = 1$.

The Hamiltonian of the isolated CQD system, H_D, is

$$H_D = \sum_{j=1,2} \varepsilon_j c_j^\dagger c_j + U c_1^\dagger c_1 c_2^\dagger c_2 + \Omega (c_1^\dagger c_2 + c_2^\dagger c_1), \tag{3}$$

where c_j is the annihilation operator for a spinless electron in the jth QD ($j=1$ and 2). ε_j is the energy of the single level in the jth QD, measured from the Fermi energy of the two electrodes at equilibrium, $\varepsilon_{1(2)} = \varepsilon_d \pm \delta$, with δ being the bare mismatch between the two bare levels. Here, we assume that only one single-electron level in each dot contributes to current. It should be noted that since we consider first-order resonant tunneling in this paper, and take no account of spin-flip scattering and spin-flip cotunneling processes (second-order tunneling processes), it is reasonable to assume spinless electrons in our model. The second term represents the interdot Coulomb interaction U. The last term of Eq. (3) denotes hopping, Ω, between the two QDs.

In this CQD system, there is a total of four possible states for the present system: (1) the whole system is empty, $|0\rangle \equiv |0\rangle_1 |0\rangle_2$, and its energy is zero; (2) the first QD is singly occupied by an electron, $|1\rangle \equiv |1\rangle_1 |0\rangle_2$, and its energy is ε_1; (3) the second QD is singly occupied, $|2\rangle \equiv |0\rangle_1 |1\rangle_2$, and its energy is ε_2; (4) both dots are occupied, $|d\rangle \equiv |1\rangle_1 |1\rangle_2$, and its energy is $\varepsilon_1 + \varepsilon_2 + U$. Furthermore, with the four possible single electronic states considered as the basis, the density-matrix elements may be expressed as $\hat{\rho}_{00} = |0\rangle\langle 0|$, $\hat{\rho}_{11} = |1\rangle\langle 1|$, $\hat{\rho}_{22} = |2\rangle\langle 2|$, $\hat{\rho}_{dd} = |d\rangle\langle d|$, and $\hat{\rho}_{12} = |1\rangle\langle 2|$. The statistical expectation values of the diagonal elements of the density matrix, $\rho_{00} = \langle \hat{\rho}_{00} \rangle$, $\rho_{jj} = \langle \hat{\rho}_{jj} \rangle$ ($j=1$ and 2), and $\rho_{dd} = \langle \hat{\rho}_{dd} \rangle$, give the occupation probabilities of the electronic levels in the system being empty, singly occupied in the jth QD by an electron, or doubly occupied by electrons, respectively. The off-diagonal term $\rho_{12} = \langle \hat{\rho}_{12} \rangle$ describes coherent superposition involving two electronic occupation states, $|1\rangle_1 |0\rangle_2$ and $|0\rangle_1 |1\rangle_2$.

To properly account for interference effects between the two pathways for tunneling through the system at hand, it is convenient to diagonalize the Hamiltonian of the isolated CQD by a unitary transformation

$$|\alpha\rangle = \cos\frac{\theta}{2}|1\rangle + \sin\frac{\theta}{2}|2\rangle, \tag{4a}$$

$$|\beta\rangle = \sin\frac{\theta}{2}|1\rangle - \cos\frac{\theta}{2}|2\rangle, \quad \theta = \arctan\frac{\Omega}{\delta}. \tag{4b}$$

The transformed Hamiltonian is

$$H_D = \lambda_\alpha |\alpha\rangle\langle\alpha| + \lambda_\beta |\beta\rangle\langle\beta| + (\varepsilon_1 + \varepsilon_2 + U)|d\rangle\langle d|, \tag{5a}$$

where $\lambda_{\alpha(\beta)}$ is the eigenenergy,

$$\lambda_{\alpha(\beta)} = \varepsilon_d \pm \Delta, \tag{5b}$$

with $\Delta = \sqrt{\Omega^2 + \delta^2}$. Correspondingly, the density-matrix elements in the new double-dot eigenstate basis, $\hat{\rho}_{\chi\chi} = |\chi\rangle\langle\chi|$ and $\hat{\rho}_{\alpha\beta} = |\alpha\rangle\langle\beta|$, have similar physical meanings to those in the site representation (SR). The relations between these density-matrix elements of singly occupied states in different bases can easily be deduced from the unitary transformation, Eq. (4). (Note that the empty state, $\hat{\rho}_{00}$, and the double occupation state, $\hat{\rho}_{dd}$, have the same meaning in both representations.)

The tunnel coupling between the interferometer and the electrodes, H_T, can be written in the eigenstate representation (ER) as ($s_\theta = \sin\frac{\theta}{2}$ and $c_\theta = \cos\frac{\theta}{2}$)

$$\begin{aligned} H_T = \sum_{\mathbf{k}} [&(V_{L1} e^{i\varphi/4} a^\dagger_{L\mathbf{k}} + V_{R1} e^{-i\varphi/4} a^\dagger_{R\mathbf{k}})(c_\theta |0\rangle\langle\alpha| + s_\theta |0\rangle\langle\beta| \\ &- s_\theta |\alpha\rangle\langle d| + c_\theta |\beta\rangle\langle d|) + (V_{L2} e^{-i\varphi/4} a^\dagger_{L\mathbf{k}} + V_{R2} e^{i\varphi/4} a^\dagger_{R\mathbf{k}}) \\ &\times (s_\theta |0\rangle\langle\alpha| - c_\theta |0\rangle\langle\beta| + c_\theta |\alpha\rangle\langle d| + s_\theta |\beta\rangle\langle d|) \\ &+ \text{H.c.}]. \end{aligned} \tag{6}$$

For simplicity, the lead-dot tunneling matrix elements, $V_{\eta j}$, are assumed to be real and independent of energy. The factor $e^{\pm i\varphi/4}$ is the accumulated Peierls phase due to the magnetic

flux Φ ($\varphi \equiv 2\pi\Phi/\Phi_0$, $\Phi_0 \equiv hc/e$ is the magnetic-flux quantum) which penetrates the area enclosed by two tunneling pathways of the interferometer.

In the following, we apply a generic quantum Langevin equation approach[30–36] to derive a set of QREs to describe the dynamics of the system variables of the CQD due to coherent resonant tunneling between external reservoirs, as modeled by Eq. (1). In the derivation, three steps are involved: First, we start from the Heisenberg equations of motion (EOMs) for the density-matrix operators $\hat{\rho}_{00}$, $\hat{\rho}_{\chi\chi'}$, and ρ_{dd} in the ER and related reservoir operators $c_{\eta\mathbf{k}}$, and then formally solve them by integration of these EOMs exactly. Next, under the assumption that the time scale of decay processes is much slower than that of free evolution, which is reasonable in the weak-tunneling approximation, we replace the time-dependent operators involved in the integrals of these EOMs approximately in terms of their free evolutions. Third, these EOMs are expanded in powers of the tunnel-coupling matrix element $V_{\eta j}$ up to second order. By adopting a Markovian approximation, we finally derive the generic QREs with arbitrary bias voltage and temperature, as well as arbitrary dot-dot hopping, as

$$\begin{aligned}\dot{\rho}_{00} = &-\left[c_\theta^2(\Gamma_{11\alpha}^{+}+\Gamma_{22\beta}^{+}) + s_\theta^2(\Gamma_{11\beta}^{+}+\Gamma_{22\alpha}^{+}) + \frac{1}{2}\sin\theta(\Gamma_{12\alpha}^{+}+\Gamma_{21\alpha}^{+}-\Gamma_{12\beta}^{+}-\Gamma_{21\beta}^{+})\right]\rho_{00}\\ &+\left[c_\theta^2\Gamma_{11\alpha}^{-}+s_\theta^2\Gamma_{22\alpha}^{-}+\frac{1}{2}\sin\theta(\Gamma_{12\alpha}^{-}+\Gamma_{21\alpha}^{-})\right]\rho_{\alpha\alpha}+\left[s_\theta^2\Gamma_{11\beta}^{-}+c_\theta^2\Gamma_{22\beta}^{-}-\frac{1}{2}\sin\theta(\Gamma_{12\beta}^{-}+\Gamma_{21\beta}^{-})\right]\rho_{\beta\beta}\\ &+\frac{1}{4}\sin\theta(\Gamma_{11\alpha}^{-}+\Gamma_{11\beta}^{-}-\Gamma_{22\alpha}^{-}-\Gamma_{22\beta}^{-})(\rho_{\alpha\beta}+\rho_{\beta\alpha})+\frac{1}{2}[s_\theta^2(\Gamma_{12\alpha}^{-}+\Gamma_{12\beta}^{-})-c_\theta^2(\Gamma_{21\alpha}^{-}+\Gamma_{21\beta}^{-})]\rho_{\alpha\beta}\\ &-\frac{1}{2}[c_\theta^2(\Gamma_{12\alpha}^{-}+\Gamma_{12\beta}^{-})-s_\theta^2(\Gamma_{21\alpha}^{-}+\Gamma_{21\beta}^{-})]\rho_{\beta\alpha},\end{aligned} \tag{7a}$$

$$\begin{aligned}\dot{\rho}_{\alpha\alpha} = &\left[c_\theta^2\Gamma_{11\alpha}^{+}+s_\theta^2\Gamma_{22\alpha}^{+}+\frac{1}{2}\sin\theta(\Gamma_{12\alpha}^{+}+\Gamma_{21\alpha}^{+})\right]\rho_{00}-\left[c_\theta^2\Gamma_{11\alpha}^{-}+s_\theta^2\Gamma_{22\alpha}^{-}+\frac{1}{2}\sin\theta(\Gamma_{12\alpha}^{-}+\Gamma_{21\alpha}^{-})\right]\rho_{\alpha\alpha}\\ &-\left[s_\theta^2\tilde{\Gamma}_{11\beta}^{+}+c_\theta^2\tilde{\Gamma}_{22\beta}^{+}-\frac{1}{2}\sin\theta(\tilde{\Gamma}_{12\beta}^{+}+\tilde{\Gamma}_{21\beta}^{+})\right]\rho_{\alpha\alpha}+\left[c_\theta^2\tilde{\Gamma}_{22\beta}^{-}+s_\theta^2\tilde{\Gamma}_{11\beta}^{-}-\frac{1}{2}\sin\theta(\tilde{\Gamma}_{12\beta}^{-}+\tilde{\Gamma}_{21\beta}^{-})\right]\rho_{dd}\\ &-\frac{1}{4}\sin\theta(\Gamma_{11\beta}^{-}-\Gamma_{22\beta}^{-}-\tilde{\Gamma}_{11\alpha}^{+}+\tilde{\Gamma}_{22\alpha}^{+})(\rho_{\alpha\beta}+\rho_{\beta\alpha})-\frac{1}{2}[s_\theta^2(\Gamma_{12\beta}^{-}-\tilde{\Gamma}_{12\alpha}^{+})-c_\theta^2(\Gamma_{21\beta}^{-}-\tilde{\Gamma}_{21\alpha}^{+})]\rho_{\alpha\beta}\\ &-\frac{1}{2}[s_\theta^2(\Gamma_{21\beta}^{-}-\tilde{\Gamma}_{21\alpha}^{+})-c_\theta^2(\Gamma_{12\beta}^{-}-\tilde{\Gamma}_{12\alpha}^{+})]\rho_{\beta\alpha},\end{aligned} \tag{7b}$$

$$\begin{aligned}\dot{\rho}_{\beta\beta} = &\left[s_\theta^2\Gamma_{11\beta}^{+}+c_\theta^2\Gamma_{22\beta}^{+}-\frac{1}{2}\sin\theta(\Gamma_{12\beta}^{+}+\Gamma_{21\beta}^{+})\right]\rho_{00}-\left[s_\theta^2\Gamma_{11\beta}^{-}+c_\theta^2\Gamma_{22\beta}^{-}-\frac{1}{2}\sin\theta(\Gamma_{12\beta}^{-}+\Gamma_{21\beta}^{-})\right]\rho_{\beta\beta}\\ &-\left[c_\theta^2\tilde{\Gamma}_{11\alpha}^{+}+s_\theta^2\tilde{\Gamma}_{22\alpha}^{+}+\frac{1}{2}\sin\theta(\tilde{\Gamma}_{12\alpha}^{+}+\tilde{\Gamma}_{21\alpha}^{+})\right]\rho_{\beta\beta}+\left[s_\theta^2\tilde{\Gamma}_{22\alpha}^{-}+c_\theta^2\tilde{\Gamma}_{11\alpha}^{-}+\frac{1}{2}\sin\theta(\tilde{\Gamma}_{12\alpha}^{-}+\tilde{\Gamma}_{21\alpha}^{-})\right]\rho_{dd}\\ &-\frac{1}{4}\sin\theta(\Gamma_{11\alpha}^{-}-\Gamma_{22\alpha}^{-}-\tilde{\Gamma}_{11\beta}^{+}+\tilde{\Gamma}_{22\beta}^{+})(\rho_{\alpha\beta}+\rho_{\beta\alpha})-\frac{1}{2}[s_\theta^2(\Gamma_{12\alpha}^{-}-\tilde{\Gamma}_{12\beta}^{+})-c_\theta^2(\Gamma_{21\alpha}^{-}-\tilde{\Gamma}_{21\beta}^{+})]\rho_{\alpha\beta}\\ &-\frac{1}{2}[s_\theta^2(\Gamma_{21\alpha}^{-}-\tilde{\Gamma}_{21\beta}^{+})-c_\theta^2(\Gamma_{12\alpha}^{-}-\tilde{\Gamma}_{12\beta}^{+})]\rho_{\beta\alpha},\end{aligned} \tag{7c}$$

$$\begin{aligned}\dot{\rho}_{dd} = &\left[s_\theta^2\tilde{\Gamma}_{11\beta}^{+}+c_\theta^2\tilde{\Gamma}_{22\beta}^{+}-\frac{1}{2}\sin\theta(\tilde{\Gamma}_{12\beta}^{+}+\tilde{\Gamma}_{21\beta}^{+})\right]\rho_{\alpha\alpha}+\left[c_\theta^2\tilde{\Gamma}_{11\alpha}^{+}+s_\theta^2\tilde{\Gamma}_{22\alpha}^{+}+\frac{1}{2}\sin\theta(\tilde{\Gamma}_{12\alpha}^{+}+\tilde{\Gamma}_{21\alpha}^{+})\right]\rho_{\beta\beta}\\ &-\left[s_\theta^2(\tilde{\Gamma}_{11\beta}^{-}+\tilde{\Gamma}_{22\alpha}^{-})+c_\theta^2(\tilde{\Gamma}_{11\alpha}^{-}+\tilde{\Gamma}_{22\beta}^{-})+\frac{1}{2}\sin\theta(\tilde{\Gamma}_{12\alpha}^{-}-\tilde{\Gamma}_{12\beta}^{-}+\tilde{\Gamma}_{21\alpha}^{-}-\tilde{\Gamma}_{21\beta}^{-})\right]\rho_{dd}\\ &-\frac{1}{4}\sin\theta(\tilde{\Gamma}_{11\alpha}^{+}+\tilde{\Gamma}_{11\beta}^{+}-\tilde{\Gamma}_{22\alpha}^{+}-\tilde{\Gamma}_{22\beta}^{+})(\rho_{\alpha\beta}+\rho_{\beta\alpha})-\frac{1}{2}[s_\theta^2(\tilde{\Gamma}_{12\alpha}^{+}+\tilde{\Gamma}_{12\beta}^{+})-c_\theta^2(\tilde{\Gamma}_{21\alpha}^{+}+\tilde{\Gamma}_{21\beta}^{+})]\rho_{\alpha\beta}\\ &+\frac{1}{2}[c_\theta^2(\tilde{\Gamma}_{12\alpha}^{+}+\tilde{\Gamma}_{12\beta}^{+})-s_\theta^2(\tilde{\Gamma}_{21\alpha}^{+}+\tilde{\Gamma}_{21\beta}^{+})]\rho_{\beta\alpha},\end{aligned} \tag{7d}$$

$$\dot{\rho}_{\alpha\beta} = i2\Delta\rho_{\alpha\beta} + \left[\frac{1}{4}\sin\theta(\Gamma^{+}_{11\alpha} + \Gamma^{+}_{11\beta} - \Gamma^{+}_{22\alpha} - \Gamma^{+}_{22\beta}) - \frac{1}{2}c_\theta^2(\Gamma^{+}_{12\alpha} + \Gamma^{+}_{12\beta}) + \frac{1}{2}s_\theta^2(\Gamma^{+}_{21\alpha} + \Gamma^{+}_{21\beta})\right]\rho_{00}$$
$$- \frac{1}{2}\left[c_\theta^2(\Gamma^{-}_{11\alpha} + \Gamma^{-}_{22\beta} + \tilde{\Gamma}^{+}_{11\alpha} + \tilde{\Gamma}^{+}_{22\beta}) + s_\theta^2(\Gamma^{-}_{11\beta} + \Gamma^{-}_{22\alpha} + \tilde{\Gamma}^{+}_{11\beta} + \tilde{\Gamma}^{+}_{22\alpha}) + \frac{1}{2}\sin\theta(\Gamma^{-}_{12\alpha} + \Gamma^{-}_{21\alpha} - \Gamma^{-}_{12\beta} - \Gamma^{-}_{21\beta} + \tilde{\Gamma}^{+}_{12\alpha}\right.$$
$$\left. + \tilde{\Gamma}^{+}_{21\alpha} - \tilde{\Gamma}^{+}_{12\beta} - \tilde{\Gamma}^{+}_{21\beta})\right]\rho_{\alpha\beta} + \frac{1}{2}\left[c_\theta^2(\Gamma^{-}_{12\alpha} - \tilde{\Gamma}^{+}_{12\beta}) - s_\theta^2(\Gamma^{-}_{21\alpha} - \tilde{\Gamma}^{+}_{21\beta}) - \frac{1}{2}\sin\theta(\Gamma^{-}_{11\alpha} - \Gamma^{-}_{22\alpha} - \tilde{\Gamma}^{+}_{11\beta} + \tilde{\Gamma}^{+}_{22\beta})\right]\rho_{\alpha\alpha}$$
$$+ \frac{1}{2}\left[c_\theta^2(\Gamma^{-}_{12\beta} - \tilde{\Gamma}^{+}_{12\alpha}) - s_\theta^2(\Gamma^{-}_{21\beta} - \tilde{\Gamma}^{+}_{21\alpha}) - \frac{1}{2}\sin\theta(\Gamma^{-}_{11\beta} - \Gamma^{-}_{22\beta} - \tilde{\Gamma}^{+}_{11\alpha} + \tilde{\Gamma}^{+}_{22\alpha})\right]\rho_{\beta\beta}$$
$$+ \frac{1}{2}\left[\frac{1}{2}\sin\theta(\tilde{\Gamma}^{-}_{22\alpha} + \tilde{\Gamma}^{-}_{22\beta} - \tilde{\Gamma}^{-}_{11\alpha} - \tilde{\Gamma}^{-}_{11\beta}) + c_\theta^2(\tilde{\Gamma}^{-}_{12\alpha} + \tilde{\Gamma}^{-}_{12\beta}) - s_\theta^2(\tilde{\Gamma}^{-}_{21\alpha} + \tilde{\Gamma}^{-}_{21\beta})\right]\rho_{dd}, \tag{7e}$$

where the electron tunneling-in(out) rates are defined as

$$\Gamma^{\pm}_{jj\chi} = \sum_\eta \Gamma^{\pm}_{\eta jj\chi} = \sum_\eta \Gamma_{\eta jj} f^{\pm}_\eta(\lambda_\chi), \tag{8a}$$

$$\Gamma^{\pm}_{12\chi} = \sum_\eta \Gamma^{\pm}_{\eta 12\chi} = \sum_\eta \Gamma_{\eta 12} e^{s_\eta i\varphi/2} f^{\pm}_\eta(\lambda_\chi), \tag{8b}$$

$$\Gamma^{\pm}_{21\chi} = \sum_\eta \Gamma^{\pm}_{\eta 21\chi} = \sum_\eta \Gamma_{\eta 12} e^{-s_\eta i\varphi/2} f^{\pm}_\eta(\lambda_\chi), \tag{8c}$$

$$\tilde{\Gamma}^{\pm}_{jj\chi} = \sum_\eta \tilde{\Gamma}^{\pm}_{\eta jj\chi} = \sum_\eta \Gamma_{\eta jj} f^{\pm}_\eta(\lambda_\chi + U), \tag{8d}$$

$$\tilde{\Gamma}^{\pm}_{12\chi} = \sum_\eta \tilde{\Gamma}^{\pm}_{\eta 12\chi} = \sum_\eta \Gamma_{\eta 12} e^{s_\eta i\varphi/2} f^{\pm}_\eta(\lambda_\chi + U), \tag{8e}$$

$$\tilde{\Gamma}^{\pm}_{21\chi} = \sum_\eta \tilde{\Gamma}^{\pm}_{\eta 21\chi} = \sum_\eta \Gamma_{\eta 12} e^{-s_\eta i\varphi/2} f^{\pm}_\eta(\lambda_\chi + U) \tag{8f}$$

[$f^{+}_\eta(\epsilon)$ is the Fermi distribution function of lead η, $f^{-}_\eta(\epsilon) = 1 - f^{+}_\eta(\epsilon)$, and $s_{L/R} = \pm 1$] with

$$\Gamma_{\eta jj'} = 2\pi\varrho_\eta V_{\eta j} V_{\eta j'} \tag{9}$$

being constant in the wide band limit (ϱ_η is the density of states of lead η). $\Gamma_{\eta jj'}$ represents the strength of tunnel coupling between the jth QD level and lead η if $j = j'$; otherwise ($j \neq j'$), it measures the interference in tunneling through the different pathways. The adjoint equation of Eq. (7e) gives the equation of motion for the RDM off-diagonal element $\rho_{\beta\alpha}$. Also, we must note the normalization relation $\rho_{00} + \Sigma_\chi \rho_{\chi\chi} + \rho_{dd} = 1$. Simple rate equations written in the ER were obtained earlier in Ref. 37 for double-well semiconductor heterostructures.

In the ER, the CQD interferometer is equivalent to a single QD with two energy levels, both of which couple to the two electrodes such that either level is tunnel coupled to either electrode via two different pathways with different tunneling matrix elements depending on differing accumulated phases due to the magnetic flux [see Eq. (6)]. Figure 3 below exhibits schematic diagrams of energy configurations for coherent tunneling through a CQD in the ER. In this situation, all tunneling events can be classified in three different categories. For example, $\Gamma^{+}_{11\alpha}$ ($\Gamma^{-}_{11\alpha}$) describes the tunneling rate of an electron entering (leaving) level α in the CQD without the occupancy of level β via pathway 1 (indicated by the upper line in Fig. 1). Similarly, $\Gamma^{+}_{22\alpha}$ ($\Gamma^{-}_{22\alpha}$) denotes the same tunneling process via pathway 2 (indicated by the lower line in Fig. 1); $\Gamma^{+}_{12\alpha}$ ($\Gamma^{-}_{12\alpha}$) describes the interferential tunneling process of an electron entering (leaving) level α without the occupancy of level β due to the interference between the two pathways 1 and 2. All $\tilde{\Gamma}^{\pm}_{jj'\chi}$ are the corresponding rates in the case of double occupation. Naturally, only the interferential tunneling term suffers an accumulated phase factor as shown in Eqs. (8b) and (8e).

Therefore, the classical parts of the dynamical equations of the RDM diagonal elements have clear classical interpretations. For example, the rate of change of electron number in level α, $\rho_{\alpha\alpha}$, in the CQD, governed by Eq. (7b), is contributed by the following four single-particle tunneling processes: (1) tunneling into level α of the CQD from both left and right leads, if the CQD is initially in the empty state ρ_{00}; (2) tunneling out from (into) level α (β) of the CQD into (from) both leads, when the CQD is initially just in the state $\rho_{\alpha\alpha}$; (3) tunneling out from level β of the CQD into both leads, when the CQD is initially in the state ρ_{dd}, via path 1, path 2, and interference contributions. The last three terms in Eq. (7b) describe transitions between two eigenstates through the effective coupling with off-diagonal elements via both paths and interference, which have no classical counterpart. They are responsible for coherent (quantum) effects in the transport. We note that even though there is no direct coupling between the two eigenstates of the isolated Hamiltonian [Eq. (5a)] in the ER, the tunnel coupling described by Eq. (6) results in an effective transition between them and, thus, leads to a quantum superposition state between the two eigenstates, whose dynamics is ruled by the equation of motion of the off-diagonal element $\rho_{\alpha\beta}$ [Eq. (7e)].

The tunneling current operator through the interferometer is defined as the time rate of change of the charge density, $N_\eta = \Sigma_{\mathbf{k}} a^{\dagger}_{\eta\mathbf{k}} a_{\eta\mathbf{k}}$, in lead η:

$$J_\eta = -\dot{N}_\eta = i[N_\eta, H]. \tag{10}$$

According to linear-response theory in the interaction picture, we have[38]

$$I_L = \langle J_L \rangle = -i\int_{-\infty}^{t} dt' \langle [J_L(t), H_I(t')]_- \rangle. \tag{11}$$

Along the same procedure as above, we arrive at the following expression for the current within the weak tunnel-coupling approximation:

$$\begin{aligned}
I_L = {} & \left[c_\theta^2(\Gamma_{L11\alpha}^+ + \Gamma_{L22\beta}^+) + s_\theta^2(\Gamma_{L11\beta}^+ + \Gamma_{L22\alpha}^+) + \frac{1}{2}\sin\theta(\Gamma_{L12\alpha}^+ + \Gamma_{L21\alpha}^+ - \Gamma_{L12\beta}^+ - \Gamma_{L21\beta}^+) \right]\rho_{00} - \left[c_\theta^2\Gamma_{L11\alpha}^- + s_\theta^2\Gamma_{L22\alpha}^- + \frac{1}{2}\sin\theta(\Gamma_{L12\alpha}^- \right. \\
& \left. + \Gamma_{L21\alpha}^-) \right]\rho_{\alpha\alpha} + \left[s_\theta^2\tilde{\Gamma}_{L11\beta}^+ + c_\theta^2\tilde{\Gamma}_{L22\beta}^- - \frac{1}{2}\sin\theta(\tilde{\Gamma}_{L12\beta}^+ + \tilde{\Gamma}_{L21\beta}^-) \right]\rho_{\alpha\alpha} - \left[s_\theta^2\Gamma_{L11\beta}^- + c_\theta^2\Gamma_{L22\beta}^- - \frac{1}{2}\sin\theta(\Gamma_{L12\beta}^- + \Gamma_{L21\beta}^-) \right]\rho_{\beta\beta} \\
& + \left[c_\theta^2\tilde{\Gamma}_{L11\alpha}^- + s_\theta^2\tilde{\Gamma}_{L22\alpha}^- + \frac{1}{2}\sin\theta(\tilde{\Gamma}_{L12\alpha}^- + \tilde{\Gamma}_{L21\alpha}^-) \right]\rho_{\beta\beta} - \frac{1}{2}\left[\frac{1}{2}\sin\theta(\Gamma_{L11\alpha}^- + \Gamma_{L11\beta}^- - \Gamma_{L22\alpha}^- - \Gamma_{L22\beta}^-) + s_\theta^2(\Gamma_{L12\alpha}^- + \Gamma_{L12\beta}^-) \right. \\
& \left. - c_\theta^2(\Gamma_{L21\alpha}^- + \Gamma_{L21\beta}^-) \right]\rho_{\alpha\beta} + \frac{1}{2}\left[\frac{1}{2}\sin\theta(\tilde{\Gamma}_{L22\alpha}^+ + \Gamma_{L22\beta}^+ - \tilde{\Gamma}_{L11\alpha}^+ - \tilde{\Gamma}_{L11\beta}^+) - s_\theta^2(\tilde{\Gamma}_{L12\alpha}^+ + \tilde{\Gamma}_{L12\beta}^+) + c_\theta^2(\tilde{\Gamma}_{L21\alpha}^+ + \tilde{\Gamma}_{L21\beta}^+) \right]\rho_{\alpha\beta} \\
& - \frac{1}{2}\left[\frac{1}{2}\sin\theta(\Gamma_{L11\alpha}^- + \Gamma_{L11\beta}^- - \Gamma_{L22\alpha}^- - \Gamma_{L22\beta}^-) - c_\theta^2(\Gamma_{L12\alpha}^- + \Gamma_{L12\beta}^-) + s_\theta^2(\Gamma_{L21\alpha}^- + \Gamma_{L21\beta}^-) \right]\rho_{\beta\alpha} \\
& + \frac{1}{2}\left[\frac{1}{2}\sin\theta(\tilde{\Gamma}_{L22\alpha}^+ + \tilde{\Gamma}_{L22\beta}^+ - \tilde{\Gamma}_{L11\alpha}^+ - \tilde{\Gamma}_{L11\beta}^+) + c_\theta^2(\tilde{\Gamma}_{L12\alpha}^+ + \tilde{\Gamma}_{L12\beta}^+) - s_\theta^2(\tilde{\Gamma}_{L21\alpha}^+ + \tilde{\Gamma}_{L21\beta}^+) \right]\rho_{\beta\alpha} \\
& - \left[s_\theta^2\tilde{\Gamma}_{L11\beta}^- + c_\theta^2\tilde{\Gamma}_{L11\alpha}^- + s_\theta^2\tilde{\Gamma}_{L22\alpha}^- + c_\theta^2\tilde{\Gamma}_{L22\beta}^- - \frac{1}{2}\sin\theta(\tilde{\Gamma}_{L12\beta}^- - \tilde{\Gamma}_{L12\alpha}^- + \tilde{\Gamma}_{L21\beta}^- - \tilde{\Gamma}_{L21\alpha}^-) \right]\rho_{dd}.
\end{aligned} \tag{12}$$

Interchanging the subscripts L and R, we obtain the tunneling current I_R relevant to the right lead. It is easy to verify that $I_L = -I_R$. This current formula demonstrates that all possible tunneling events relevant to lead η (tunneling through both paths and with the interferential term) provide corresponding contributions to the current of lead η; the current is determined not only by the RDM diagonal elements, but it also involves the off-diagonal elements explicitly.

Another observable of interest is the current noise, whose spectrum is defined as the Fourier transform of the symmetric current-current correlation function

$$S_{\eta\eta'}(\omega) = \int_{-\infty}^{\infty} d\tau e^{i\omega\tau}\frac{1}{2}\langle [\delta J_\eta(t), \delta J_{\eta'}(t')]_+ \rangle, \tag{13}$$

with $\delta J_\eta(t) = J_\eta(t) - I_\eta$. Here, we only consider the frequency-independent (Schottky-type) shot noise. Employing linear-response theory, we can also evaluate its statistical expectation value to the first nonvanishing term in H_I, obtaining

$$\begin{aligned}
S_{LL} = \frac{1}{2}\int_{-\infty}^{\infty} d\tau \langle [J_L^o(t), J_L^o(t')]_+ \rangle = {} & \left[c_\theta^2(\Gamma_{L11\alpha}^+ + \Gamma_{L22\beta}^+) + s_\theta^2(\Gamma_{L11\beta}^+ + \Gamma_{L22\alpha}^+) + \frac{1}{2}\sin\theta(\Gamma_{L12\alpha}^+ + \Gamma_{L21\alpha}^+ - \Gamma_{L12\beta}^+ - \Gamma_{L21\beta}^+) \right]\rho_{00} \\
& + \left[c_\theta^2\Gamma_{L11\alpha}^- + s_\theta^2\Gamma_{L22\alpha}^- + \frac{1}{2}\sin\theta(\Gamma_{L12\alpha}^- + \Gamma_{L21\alpha}^-) \right]\rho_{\alpha\alpha} + \left[s_\theta^2\tilde{\Gamma}_{L11\beta}^+ + c_\theta^2\tilde{\Gamma}_{L22\beta}^- - \frac{1}{2}\sin\theta(\tilde{\Gamma}_{L12\beta}^+ + \tilde{\Gamma}_{L21\beta}^-) \right]\rho_{\alpha\alpha} \\
& + \left[s_\theta^2\Gamma_{L11\beta}^- + c_\theta^2\Gamma_{L22\beta}^- - \frac{1}{2}\sin\theta(\Gamma_{L12\beta}^- + \Gamma_{L21\beta}^-) \right]\rho_{\beta\beta} + \left[c_\theta^2\tilde{\Gamma}_{L11\alpha}^- + s_\theta^2\tilde{\Gamma}_{L22\alpha}^- + \frac{1}{2}\sin\theta(\tilde{\Gamma}_{L12\alpha}^- + \tilde{\Gamma}_{L21\alpha}^-) \right]\rho_{\beta\beta} \\
& + \frac{1}{2}\left[\frac{1}{2}\sin\theta(\Gamma_{L11\alpha}^- + \Gamma_{L11\beta}^- - \Gamma_{L22\alpha}^- - \Gamma_{L22\beta}^-) + s_\theta^2(\Gamma_{L12\alpha}^- + \Gamma_{L12\beta}^-) - c_\theta^2(\Gamma_{L21\alpha}^- + \Gamma_{L21\beta}^-) \right]\rho_{\alpha\beta} + \frac{1}{2}\left[\frac{1}{2}\sin\theta(\tilde{\Gamma}_{L22\alpha}^+ + \Gamma_{L22\beta}^+ \right. \\
& \left. - \tilde{\Gamma}_{L11\alpha}^+ - \tilde{\Gamma}_{L11\beta}^+) - s_\theta^2(\tilde{\Gamma}_{L12\alpha}^+ + \tilde{\Gamma}_{L12\beta}^+) + c_\theta^2(\tilde{\Gamma}_{L21\alpha}^+ + \tilde{\Gamma}_{L21\beta}^+) \right]\rho_{\alpha\beta} + \frac{1}{2}\left[\frac{1}{2}\sin\theta(\Gamma_{L11\alpha}^- + \Gamma_{L11\beta}^- - \Gamma_{L22\alpha}^- - \Gamma_{L22\beta}^-) - c_\theta^2(\Gamma_{L12\alpha}^- \right. \\
& \left. + \Gamma_{L12\beta}^-) + s_\theta^2(\Gamma_{L21\alpha}^- + \Gamma_{L21\beta}^-) \right]\rho_{\beta\alpha} + \frac{1}{2}\left[\frac{1}{2}\sin\theta(\tilde{\Gamma}_{L22\alpha}^+ + \tilde{\Gamma}_{L22\beta}^+ - \tilde{\Gamma}_{L11\alpha}^+ - \tilde{\Gamma}_{L11\beta}^+) + c_\theta^2(\tilde{\Gamma}_{L12\alpha}^+ + \tilde{\Gamma}_{L12\beta}^+) - s_\theta^2(\tilde{\Gamma}_{L21\alpha}^+ + \tilde{\Gamma}_{L21\beta}^+) \right]\rho_{\beta\alpha} \\
& + \left[s_\theta^2\tilde{\Gamma}_{L11\beta}^- + c_\theta^2\tilde{\Gamma}_{L11\alpha}^- + s_\theta^2\tilde{\Gamma}_{L22\alpha}^- + c_\theta^2\tilde{\Gamma}_{L22\beta}^- - \frac{1}{2}\sin\theta(\tilde{\Gamma}_{L12\beta}^- - \tilde{\Gamma}_{L12\alpha}^- + \tilde{\Gamma}_{L21\beta}^- - \tilde{\Gamma}_{L21\alpha}^-) \right]\rho_{dd}.
\end{aligned} \tag{14}$$

The corresponding result for S_{RR} is obtained by interchanging the subscripts L and R in Eq. (14). In leading order, $S_{LR}=S_{RL}=0$.

This shot noise formula merits further discussion. It is well known that the Schottky noise originates from the self-correlation of a given tunneling event with itself. In literature, this term has been elaborately studied for a sequential picture of resonant tunneling through a double-barrier transistor using a master equation,[39,40] and also using a stochastic wave function approach.[41] These previous studies show that the classical intrinsic shot noise can simply be expressed by the formula[39,40]

$$S_{\eta\eta}=\sum_n (+)\gamma_{\eta n}\boldsymbol{\rho}_n^0, \tag{15a}$$

provided the current can be written in the following form:

$$I_\eta=\sum_n (+/-)\gamma_{\eta n}\boldsymbol{\rho}_n^0, \tag{15b}$$

where $\boldsymbol{\rho}$ is a vector whose components are the RDM elements of the single-electron transistor, the superscript "0" indicates its stationary solution based on the rate equation, and $\gamma_{\eta n}$ is the corresponding rate of a possible tunneling process that can change the state n of the single-electron transistor and contribute to the current of lead η. This is to say that all single-particle tunneling processes involving lead η will give a positive (+) or a negative (−) contribution to the current of lead η, depending on whether an electron is to enter or to leave this lead in a particular tunneling process; nevertheless, self-correlation terms in all these same processes will always result in a positive (+) contribution to the Schottky-type shot noise, and the only difference between the current and the self-correlation noise formulas [Eqs. (15b) and (15a)] is a sign change. We note that Eq. (15a) has only been proved for a classical double-barrier tunneling device, in which the RDM of the device has only diagonal elements (thus, $\boldsymbol{\rho}_n^0 \geqslant 0$) and the tunneling rate $\gamma_{\eta n}$ is always non-negative ($\gamma_{\eta n}\geqslant 0$). Without attempting to rigorously verify its validity, this scheme has been recently applied directly to calculate the Schottky-type shot noise of a QD system having coupled internal degrees of freedom, but with its current being explicitly dependent only on RDM diagonal elements which always have positive values.[24,25] The present theoretical formulation circumvents this problem. Furthermore, we prove here that (1) this scheme is just a result of linear-response theory in the weak-tunneling limit, and (2) this scheme remains valid for the calculation of Schottky-type shot noise of a CQD interferometer, for which not only RDM diagonal elements contribute to the current, but also off-diagonal elements, with stationary values and corresponding tunneling rates which could possibly be both negative.

III. COUPLED QUANTUM DOT IN A SERIES CONFIGURATION

In this section, we discuss coherent resonant tunneling through a series CQD in the case of infinite interdot Coulomb repulsion, $U=\infty$. In this case, the corresponding tunneling amplitudes and the interferential tunneling vanish, $\Gamma_{L22}=\Gamma_{R11}=0$, $\Gamma_{L12}=\Gamma_{R12}=0$, and all $\tilde{\Gamma}=0$. We also choose $\delta=0$ ($\varepsilon_1=\varepsilon_2=\varepsilon_d$).

For comparison with our previous QREs in the case of weak interdot hopping,[18] we reexpress the resulting generic QREs [Eqs. (7a)–(7e)] in the SR for the case of a series configuration ($\Gamma_{L\chi}^{\pm}=\Gamma_{L11\chi}^{\pm}$ and $\Gamma_{R\chi}^{\pm}=\Gamma_{R22\chi}^{\pm}$):

$$\dot{\rho}_{00}=-(\tilde{\Gamma}_L^+ + \tilde{\Gamma}_R^+)\rho_{00}+\tilde{\Gamma}_L^-\rho_{11}+\tilde{\Gamma}_R^-\rho_{22} + \frac{1}{4}\sin\theta(\Gamma_{L\alpha}^- + \Gamma_{R\alpha}^- - \Gamma_{L\beta}^- - \Gamma_{R\beta}^-)(\rho_{12}+\rho_{21}), \tag{16a}$$

$$\dot{\rho}_{11}=\tilde{\Gamma}_L^+\rho_{00}-\tilde{\Gamma}_L^-\rho_{11}+i\Omega(\rho_{21}-\rho_{12}) - \frac{1}{4}\sin\theta(\Gamma_{L\alpha}^- - \Gamma_{L\beta}^-)(\rho_{12}+\rho_{21}), \tag{16b}$$

$$\dot{\rho}_{22}=\tilde{\Gamma}_R^+\rho_{00}-\tilde{\Gamma}_R^-\rho_{22}-i\Omega(\rho_{21}-\rho_{12}) - \frac{1}{4}\sin\theta(\Gamma_{R\alpha}^- - \Gamma_{R\beta}^-)(\rho_{12}+\rho_{21}), \tag{16c}$$

$$\dot{\rho}_{12}=i2\delta\rho_{12}-i\Omega(\rho_{11}-\rho_{22})-\frac{1}{2}(\tilde{\Gamma}_L^- + \tilde{\Gamma}_R^-)\rho_{12} + \frac{1}{4}\sin\theta(\Gamma_{L\alpha}^+ + \Gamma_{R\alpha}^+ - \Gamma_{L\beta}^+ - \Gamma_{R\beta}^+)\rho_{00} - \frac{1}{4}\sin\theta(\Gamma_{R\alpha}^- - \Gamma_{R\beta}^-)\rho_{11} - \frac{1}{4}\sin\theta(\Gamma_{L\alpha}^- - \Gamma_{L\beta}^-)\rho_{22}, \tag{16d}$$

with $\rho_{00}+\rho_{11}+\rho_{22}=1$ and $\rho_{21}=\rho_{12}^*$, in which

$$\tilde{\Gamma}_L^{\pm}=c_\theta^2\Gamma_{L\alpha}^{\pm}+s_\theta^2\Gamma_{L\beta}^{\pm} \tag{16e}$$

and

$$\tilde{\Gamma}_R^{\pm}=s_\theta^2\Gamma_{R\alpha}^{\pm}+c_\theta^2\Gamma_{R\beta}^{\pm}, \tag{16f}$$

denote the effective tunneling rates between the first (second) dot and the left (right) lead. The current becomes

$$I_L=\tilde{\Gamma}_L^+\rho_{00}-\tilde{\Gamma}_L^-\rho_{11}-\frac{1}{4}\sin\theta(\Gamma_{L\alpha}^- - \Gamma_{L\beta}^-)(\rho_{12}+\rho_{21}). \tag{17}$$

Comparing with our previous results [Eqs. (39a)–(39c) of Ref. 18], we find some different features in our present QREs [Eqs. (16a)–(16d)] in the SR: (1) The tunneling rates between dot and lead, $\tilde{\Gamma}_{L/R}^{\pm}$, are modified to account for the effect of interdot hopping. (2) More interestingly, effective interdot hopping induced by tunneling to external electrodes provides a different contribution, which is dependent on the real part of the RDM off-diagonal elements, to the dynamics of the RDM diagonal elements stemming from quantum coherence [for instance, the fourth terms on the right hand side (rhs) of Eqs. (16b) and (16c)]. (3) Conversely, this effective

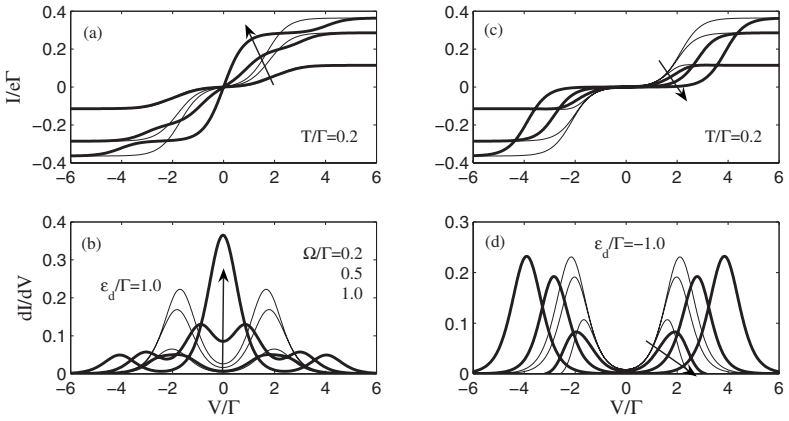

FIG. 2. [(a) and (c)] Average current and [(b) and (d)] the differential conductance vs bias voltage with several different interdot hopping strengths $\Omega/\Gamma=0.2$, 0.5, and 1.0. (a) and (b) are plotted for $\varepsilon_d/\Gamma=1.0$, (c) and (d) for $\varepsilon_d/\Gamma=-1.0$. The thick lines denote the results calculated by the present QREs [Eqs. (16a)–(16d) and (17)], while the thin lines arise from the previous QREs [Eqs. (39a)–(39c) in Ref. 18]. The temperature is fixed as $T/\Gamma=0.2$.

interdot hopping also leads to a different damping of quantum superposition related to the diagonal elements themselves, as shown by the final three terms on the rhs of Eq. (16d). Moreover, the real part of the off-diagonal elements makes an explicit, direct contribution to the tunneling current and Schottky-type shot noise.

In regard to the fact that our previous QREs are only valid for the case of weak interdot hopping, whereas our present QREs are derived without that limitation, it is interesting to note that the present generic QREs do reduce to the previous QREs in the limit $\Omega\to 0$ ($\ll\Gamma_{L/R}$). In this situation, from Eq. (5b) we have $\lambda_{\alpha(\beta)}=\varepsilon_d\pm\Omega$ ($\delta=0$), leading to $\lambda_\alpha\approx\lambda_\beta$ and, thus, $\Gamma^{\pm}_{\eta\alpha}\approx\Gamma^{\pm}_{\eta\beta}$. This approximate relation eliminates the additional quantum coherence terms of Eqs. (16a)–(16d) due to the tunneling-induced effective dot-dot hopping, and, consequently, the QREs reduce exactly to our previous results. For numerical verification of this assertion, we examine the effect of hopping ($\Omega/\Gamma=0.2-1.0$) on resonant tunneling in Fig. 2, where we plot the average current I, and the differential conductance dI/dV, as functions of bias voltage for two cases, $\varepsilon_d/\Gamma=1.0$ and -1.0. Hereafter, we choose a completely symmetric geometry, $\Gamma_{L11}=\Gamma_{R22}=\Gamma$, and use Γ as the unit of energy, and the current is normalized to $\frac{e}{\hbar}\Gamma$. We exhibit the calculated results using the present QREs [Eqs. (16b)–(16d)] by the thick lines and those of the previous QREs [Eqs. (39a)–(39c) in Ref. 18] by the thin lines.

It is obvious that there is no nontrivial difference in the separate calculations for these physical quantities in the case of weakest dot-dot hopping, $\Omega/\Gamma=0.2$. With increasing dot-dot hopping, the difference between the two theories becomes unambiguous and cannot be ignored. In particular, a zero-bias peak in the differential conductance, dV/dI, is found by the present theory for the system of $\varepsilon_d/\Gamma=1.0$ with dot-dot hopping $\Omega/\Gamma=1.0$, in contrast to the peak splitting around zero-bias voltage predicted by the previous QREs. On the other hand, for the system of $\varepsilon_d/\Gamma=-1.0$, both calculated results for differential conductance show a peak-splitting structure, but they have different splitting widths. The transport properties are clearly asymmetric between the systems with $\varepsilon_d>0$ and $\varepsilon_d<0$, which have already been pointed out in linear transport regime.[9] In fact, this asymmetric feature can be easily explained by examining the energetic structure of the present system. As mentioned above, the CQD in the ER can be mapped onto a model of a single QD with two levels, α and β, each connecting to both electrodes with different tunneling matrix elements. The physical picture is illustrated in Fig. 3, which includes a total of six configurations [(a)–(f)], showing the relative relations among the two eigenenergies and the Fermi energies of the two electrodes. For simplicity, we set $T=0$ in the following analysis. In configurations (a) and (d), the CQD is always singly occupied by an electron, while it is always empty in configuration (b). The three cases have all vanishing first-order tunneling current and current noise because the two eigenlevels are both far away from resonance with the Fermi levels of the two electrodes. On the contrary, both eigenlevels are in resonance with the Fermi levels of the electrodes in configuration (c), which is actually equivalent to a picture of resonant tunneling under extremely large bias voltage. It is, therefore, not unexpected that the resulting rates and current in this case are identical to the results obtained by Gurvitz and Prager for the same system,[16] as well as matching our previous results for the same conditions.[18]

Moreover, it is quite surprising that the current is also zero in the resonant configuration (e). We can ascribe this

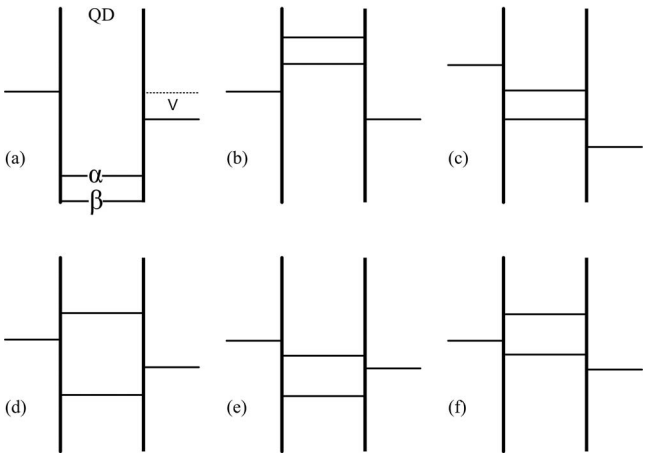

FIG. 3. Schematic energetic configurations for coherent tunneling through a CQD in the ER. The CQD behaves as a single QD with two levels α and β, both of which are coupled to both the left and right leads. In configurations (a)–(c), the additional quantum coherence terms automatically vanish in the QREs (16a)–(16d) and in the current formula (17), while in (d)–(f), they play an important role in tunneling.

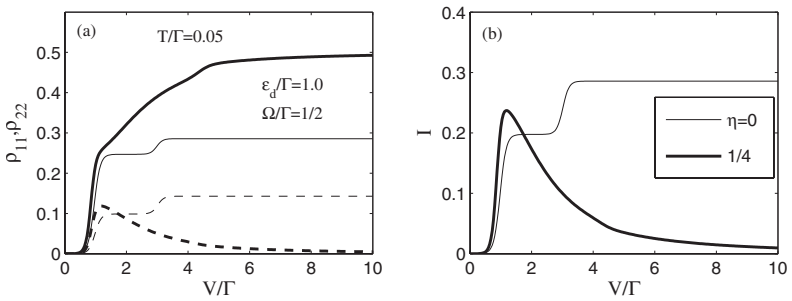

FIG. 4. (a) Occupation numbers ρ_{11} (solid lines), ρ_{22} (dashed lines) and (b) average current vs bias voltage, with the bias-voltage-induced shifting factor $\eta=0$ (thin lines) and $1/4$ (thick lines) for $\varepsilon_d/\Gamma=1.0$, $\Omega/\Gamma=1/2$, and $T/\Gamma=0.05$.

result to the strong Coulomb blockade effect, which blocks the entry of an additional electron into the singly occupied CQD even though the upper eigenlevel is in resonance with the Fermi levels of the electrodes. The situation is different in configuration (f), in which only the lower eigenlevel is in resonance with the Fermi levels of two leads and, thus, a nonzero current occurs. We note that this current is always smaller than the current in configuration (c). [This is only true for a series CQD, while for a parallel CQD, the situation may be opposite (see below).] Actually, configuration (f) describes a picture of resonant tunneling under a small bias voltage, in contrast to the case of large bias voltage in configuration (c).

It should be noted that our present QREs are also applicable for the cases with a detuning of the bare level energies, i.e., $\delta\neq 0$. Actually, spatial variation of bias voltage on the series CQD is quite a central issue in the present studies.[42–44] Without loss of generality, we assume that the bare QD energies are shifted by the bias voltage as $\varepsilon_{1(2)}=\varepsilon_d \pm \eta V$, and assume further that one-fourth of the applied voltage drops at the contacts between the QDs and the leads, i.e., the bias-voltage-induced shifting factor $\eta=1/4$. As an illustration, we exhibit the effects of energy shifting on the electron occupation numbers of two QDs and the current in Fig. 4. It is found that the main effect of the spatially varying electric field is to cause an appearance of negative differential conductance (NDC) in the current-voltage characteristics, which has been reported previously by nonequilibrium Green's function calculations[43] in order to explain the experimental results in the Tour molecules.[45] Here, we can give a simple interpretation for the appearance of NDC as follows: Due to the spatial variation of bias voltage, the eigenenergies for the CQD become voltage dependent, $\lambda_{\alpha(\beta)}=\varepsilon_d \pm \sqrt{\Omega^2+\eta^2 V^2}$. This dependence remarkably modifies the electronic occupation behavior in comparison with the no shifting case. Electrons have more opportunity to occupy the first QD for large bias voltages, leading to a decrease of the occupation number of the second QD, ρ_{22}, with increasing bias voltage as shown in Fig. 4(a), which is the reason for the appearance of NDC, because the nonequilibrium current is dominatively dependent on the occupation number of the second QD in the series configuration.

IV. COUPLED QUANTUM DOT IN A PARALLEL CONFIGURATION

Focusing attention on the case of resonant tunneling through a parallel CQD, we again choose the optimal resonant condition, $\delta=0$, and we also assume the tunneling constants as $\Gamma_{L11}=\Gamma_{R22}=\Gamma$ and $\Gamma_{L22}=\Gamma_{R11}=\Gamma'$, thus $\Gamma_{L12}=\Gamma_{R12}=\sqrt{\Gamma\Gamma'}$, which yield

$$\Gamma^{\pm}_{11\chi}=\Gamma f^{\pm}_L(\lambda_\chi)+\Gamma' f^{\pm}_R(\lambda_\chi), \tag{18a}$$

$$\Gamma^{\pm}_{22\chi}=\Gamma' f^{\pm}_L(\lambda_\chi)+\Gamma f^{\pm}_R(\lambda_\chi), \tag{18b}$$

$$\Gamma^{\pm}_{12\chi}=\sqrt{\Gamma\Gamma'}[e^{i\varphi/2}f^{\pm}_L(\lambda_\chi)+e^{-i\varphi/2}f^{\pm}_R(\lambda_\chi)], \tag{18c}$$

$$\Gamma^{\pm}_{21\chi}=\sqrt{\Gamma\Gamma'}[e^{-i\varphi/2}f^{\pm}_L(\lambda_\chi)+e^{i\varphi/2}f^{\pm}_R(\lambda_\chi)]. \tag{18d}$$

At first, we consider the case of $U\to\infty$. If dot-dot hopping vanishes, i.e., $\Omega=0$, the QREs coincide with our previous results in Ref. 46.

A. Simplified quantum rate equations in the site representation for configurations (c) and (f)

The energetic configurations for coherent tunneling through a CQD interferometer are also depicted in Fig. 3. Analogous to the series CQD, only configurations (c) and (f) bear nonzero tunneling current for the present parallel arrangement. For reference purposes, we therefore provide the simplified QREs written in the SR at zero temperature for these two configurations below.

For an extremely large bias voltage [configuration (c)], these tunneling rates simplify further as $\Gamma^{+}_{11\alpha(\beta)}=\Gamma^{-}_{22\alpha(\beta)}=\Gamma$, $\Gamma^{+}_{22\alpha(\beta)}=\Gamma^{-}_{11\alpha(\beta)}=\Gamma'$, $\Gamma^{+}_{12\alpha(\beta)}=\Gamma^{-}_{21\alpha(\beta)}=\sqrt{\Gamma\Gamma'}e^{i\varphi/2}$, and $\Gamma^{-}_{12\alpha(\beta)}=\Gamma^{+}_{21\alpha(\beta)}=\sqrt{\Gamma\Gamma'}e^{-i\varphi/2}$. The simplified QREs in terms of the SR finally become

$$\dot{\rho}_{00}=\Gamma'\rho_{11}+\Gamma\rho_{22}-(\Gamma+\Gamma')\rho_{00}+\sqrt{\Gamma\Gamma'}(e^{i\varphi/2}\rho_{12}+e^{-i\varphi/2}\rho_{21}), \tag{19a}$$

$$\dot{\rho}_{11}=\Gamma\rho_{00}-\Gamma'\rho_{11}+i\Omega(\rho_{21}-\rho_{12})-\frac{1}{2}\sqrt{\Gamma\Gamma'}(e^{i\varphi/2}\rho_{12}+e^{-i\varphi/2}\rho_{21}), \tag{19b}$$

$$\dot{\rho}_{22}=\Gamma'\rho_{00}-\Gamma\rho_{22}-i\Omega(\rho_{21}-\rho_{12})-\frac{1}{2}\sqrt{\Gamma\Gamma'}(e^{i\varphi/2}\rho_{12}+e^{-i\varphi/2}\rho_{21}), \tag{19c}$$

$$\dot{\rho}_{12} = i2\delta\rho_{12} - i\Omega(\rho_{11} - \rho_{22}) - \frac{1}{2}(\Gamma + \Gamma')\rho_{12} + \sqrt{\Gamma\Gamma'}e^{i\varphi/2}\rho_{00} - \frac{1}{2}\sqrt{\Gamma\Gamma'}e^{-i\varphi/2}(\rho_{11} + \rho_{22}), \tag{19d}$$

along with the normalization relation, $\rho_{00}+\rho_{11}+\rho_{22}=1$ and $\rho_{21}=\rho_{12}^{*}$. As expected, we note that the resulting QREs [Eqs. (19a)–(19d)] coincide with those of our previous derivation for the same system analyzed in Ref. 13. The current becomes

$$I_L = (\Gamma + \Gamma')\rho_{00},$$

$$I_R = -[\Gamma'\rho_{11} + \Gamma\rho_{22} + \sqrt{\Gamma\Gamma'}(e^{i\varphi/2}\rho_{12} + e^{-i\varphi/2}\rho_{21})]. \tag{20}$$

Moreover, the system of configuration (f) yields

$$\dot{\rho}_{11} = \left(\Gamma s_\theta^2 - \frac{1}{2}\sqrt{\Gamma\Gamma'}\sin\theta\cos\frac{\varphi}{2}\right)\rho_{00} + i\Omega(\rho_{21} - \rho_{12}) - \left(\Gamma' + \Gamma c_\theta^2 + \frac{1}{2}\sqrt{\Gamma\Gamma'}\sin\theta\cos\frac{\varphi}{2}\right)\rho_{11} - \frac{1}{2}\sqrt{\Gamma\Gamma'}(e^{i\varphi/2}\rho_{12} + e^{-i\varphi/2}\rho_{21}) - \frac{1}{2}\sqrt{\Gamma\Gamma'}s_\theta^2(e^{-i\varphi/2}\rho_{12} + e^{i\varphi/2}\rho_{21}) - \frac{1}{4}\Gamma\sin\theta(\rho_{12} + \rho_{21}), \tag{21a}$$

$$\dot{\rho}_{22} = \left(\Gamma' c_\theta^2 - \frac{1}{2}\sqrt{\Gamma\Gamma'}\sin\theta\cos\frac{\varphi}{2}\right)\rho_{00} - i\Omega(\rho_{21} - \rho_{12}) - \left(\Gamma + \Gamma' s_\theta^2 + \frac{1}{2}\sqrt{\Gamma\Gamma'}\sin\theta\cos\frac{\varphi}{2}\right)\rho_{22} - \frac{1}{2}\sqrt{\Gamma\Gamma'}(e^{i\varphi/2}\rho_{12} + e^{-i\varphi/2}\rho_{21}) - \frac{1}{2}\sqrt{\Gamma\Gamma'}c_\theta^2(e^{-i\varphi/2}\rho_{12} + e^{i\varphi/2}\rho_{21}) - \frac{1}{4}\Gamma'\sin\theta(\rho_{12} + \rho_{21}), \tag{21b}$$

$$\dot{\rho}_{12} = 2i\delta\rho_{12} - i\Omega(\rho_{11} - \rho_{22}) - \frac{1}{2}[\sqrt{\Gamma\Gamma'}\sin\theta e^{i\varphi/2} + \Gamma'(s_\theta^2 + 1) + \Gamma(c_\theta^2 + 1)]\rho_{12} + \left[\frac{1}{2}\sqrt{\Gamma\Gamma'}e^{i\varphi/2} - \frac{1}{4}(\Gamma + \Gamma')\sin\theta\right]\rho_{00} - \frac{1}{2}\sqrt{\Gamma\Gamma'}e^{-i\varphi/2}(\rho_{11} + \rho_{22}) - \frac{1}{2}\sqrt{\Gamma\Gamma'}c_\theta^2 e^{i\varphi/2}\rho_{11} - \frac{1}{4}\Gamma'\sin\theta\rho_{11} - \frac{1}{2}\sqrt{\Gamma\Gamma'}s_\theta^2 e^{i\varphi/2}\rho_{22} - \frac{1}{4}\Gamma\sin\theta\rho_{22}. \tag{21c}$$

The simplified current expressed in the ER is given by

$$I_L = 2[c_\theta^2\Gamma' + s_\theta^2\Gamma - \sqrt{\Gamma\Gamma'}\sin\theta\cos(\varphi/2)]\rho_{00} - 2[c_\theta^2\Gamma + s_\theta^2\Gamma' + \sqrt{\Gamma\Gamma'}\sin\theta\cos(\varphi/2)]\rho_{\alpha\alpha} - \left[\frac{1}{2}(\Gamma - \Gamma')\sin\theta + s_\theta^2\sqrt{\Gamma\Gamma'}e^{i\varphi/2} - c_\theta^2\sqrt{\Gamma\Gamma'}e^{-i\varphi/2}\right]\rho_{\alpha\beta} - \left[\frac{1}{2}(\Gamma - \Gamma')\sin\theta - c_\theta^2\sqrt{\Gamma\Gamma'}e^{i\varphi/2} + s_\theta^2\sqrt{\Gamma\Gamma'}e^{-i\varphi/2}\right]\rho_{\beta\alpha}, \tag{22}$$

which is useful for the analysis of the AB interference effect in this configuration.

B. Calculations and discussion: Aharonov-Bohm interference effect between two pathways

Below, we present numerical analyses for first-order resonant tunneling through a CQD interferometer based on the QREs of Eqs. (7a)–(7e), and the current formula [Eq. (12)]. To start, we emphasize the interference effect on tunneling due to the additional pathway. As an illustration, we carry out calculations by changing the tunnel-coupling strength Γ' of the additional path from 0 (the series configuration) to Γ (the completely symmetrical parallel configuration), as shown in Fig. 5 for two cases, $\varepsilon_d/\Gamma=1.0$ and -1.0, respectively, in the absence of magnetic flux, $\varphi=0$.

We note that the interference effect significantly changes transport properties when the system is in configuration (f) for $\varepsilon_d/\Gamma>0$, while it has little influence on tunneling when $\varepsilon_d/\Gamma<0$. This asymmetry of the interference pattern is also due to strong interaction. As displayed in Fig. 5(c), the eigenlevel β is always singly occupied in configurations (a) and (e), which blocks entry of an additional electron to the CQD, leading to vanishing current, irrespective of whether the additional tunnel path is available or not. Increasing the tunnel rate Γ' of the additional pathway suppresses the current until it entirely vanishes in the case of a completely symmetrical parallel geometry, $\Gamma'=\Gamma$, for the bias-voltage window $3>|V/\Gamma|>1$ of the system with $\varepsilon_d/\Gamma=1.0$ and $\Omega/\Gamma=1/2$ [configuration (f)] as depicted in Fig. 5(a). Accordingly, the differential conductance finally develops a two-peak structure located at the bias-voltage values, separating configurations (f) and (c) with an enhanced peak height [Fig. 5(b)]. This behavior can be intuitively interpreted as a result of perfectly destructive quantum interference between the additional pathway and the original one for configuration (f).

C. Finite-bias-induced Aharonov-Bohm oscillations and magnetic-flux-induced negative differential conductance

In this section, we examine the magnetic-flux dependence of coherent tunneling through the parallel CQD. Above, we found that nonzero tunneling current occurs only for configurations (f) (finite bias voltage) and (c) (infinite bias voltage). We consider these two cases.

We determine the nonequilibrium dot occupations $\rho_{11(22)}$ and tunneling current I based on the simplified QREs of Sec. IV A. The calculated results are illustrated in Fig. 6 for a CQD with $\Gamma'/\Gamma=0.5$ and $\Omega/\Gamma=0.5$. Clearly, the dot occupations exhibit periodic oscillations with period 4π for both cases. Actually, our previous studies have already shown that interdot hopping yields periodicity of the AB oscillation as 4π.[13] We further observe that $\rho_{11}\sim\sin(\varphi/2)$ and $\rho_{22}\sim-\sin(\varphi/2)$ for configuration (c), leading to a magnetic-flux-independent result for $\rho_{00}=1-2(\rho_{11}+\rho_{22})$. Since I/Γ

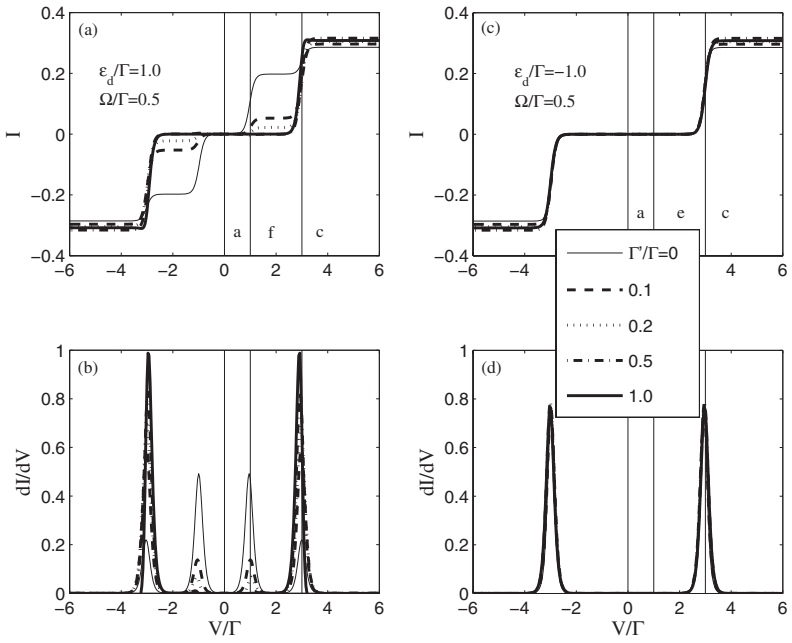

FIG. 5. [(a) and (c)] The average current and [(b) and (d)] the differential conductance $\frac{dI}{dV}$ vs bias voltage for several increasing tunnel-coupling strength values $\Gamma'/\Gamma=0$, 0.1, 0.2, 0.5, and 1.0 of the additional path without magnetic flux, $\varphi=0$, for the systems with [(a) and (b)] $\varepsilon_d/\Gamma=1.0$ and [(c) and (d)] $\varepsilon_d/\Gamma=-1.0$. Other parameters are $\Omega/\Gamma=0.5$ and $T/\Gamma=0.05$.

$\sim\rho_{00}$ [Eq. (20)], the current of configuration (c) is consequently independent of magnetic flux, as shown in Fig. 6(b). This result is quite surprising. In fact, if dissipative mechanisms are considered, ρ_{22} may not be completely out of phase with ρ_{11} (i.e., partial interference), thus the current of configuration (c) could become a periodic function of magnetic flux.

The current of configuration (f) is complex according to Eq. (22). The results of the preceding section show that perfectly destructive quantum interference causes the current to vanish for zero magnetic flux, $\varphi=0$, in this configuration

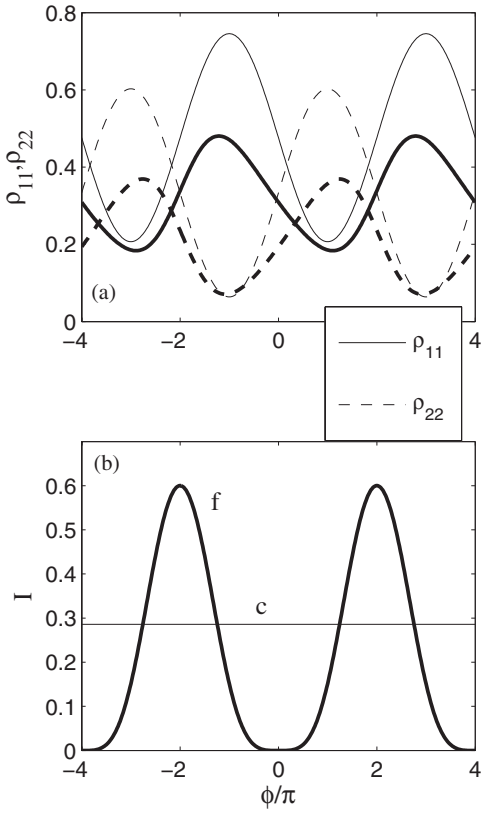

FIG. 6. Calculated magnetic-flux dependence of (a) the dot occupations ρ_{11} and ρ_{22} and (b) the tunneling current for a CQD with $\Gamma'/\Gamma=0.5$ and $\Omega/\Gamma=0.5$ in configurations (c) (thin lines) and (f) (thick lines), respectively.

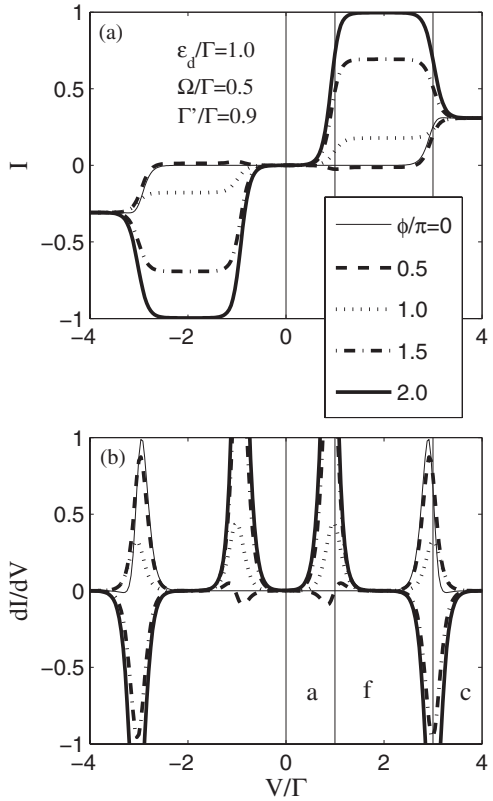

FIG. 7. (a) Calculated tunneling current I and (b) differential conductance $\frac{dI}{dV}$ for a CQD with $\Gamma'/\Gamma=0.9$, $\varepsilon_d/\Gamma=1.0$, and $\Omega/\Gamma=0.5$ for various magnetic fluxes ($\varphi/\pi=0$, 0.5, 1.0, 1.5, and 2.0). The temperature is $T/\Gamma=0.05$.

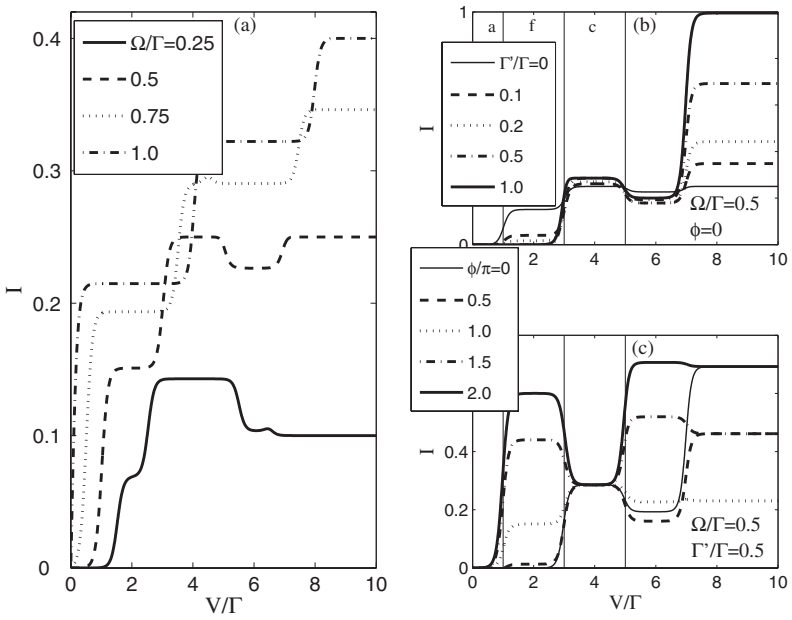

FIG. 8. Bias-dependent tunneling current I (a) for a series CQD with various dot-dot hoppings and for a parallel CQD as functions of (b) Γ' and (c) magnetic flux. The interdot Coulomb repulsion is set as $U=2\Gamma$, and other parameters are $\varepsilon_d/\Gamma=1.0$ and $T/\Gamma=0.05$.

[Fig. 5(a)]. Application of a magnetic field will induce variation of the interference effect from a destructive pattern to a constructive one. Therefore, one can expect that the enclosed magnetic flux, $\varphi=\pm 2\pi$, will enhance the current due to perfectly constructive interference. A striking result we obtain is that the enhanced current may be much larger than the constant current of configuration (c), indicating the appearance of a NDC at the boundary between configurations (f) and (c). The variation of the I-V characteristic and differential conductance with varying magnetic flux is shown in Fig. 7.

D. Finite interdot Coulomb repulsion U

Here, we examine the transport of a CQD in the case of weak dot-dot Coulomb interaction, $U=2\Gamma$.

Figure 8(a) plots the calculated current for a series CQD with $\varepsilon_d/\Gamma=1.0$ and various interdot hoppings, $\Omega/\Gamma=0.25-1.0$. Different from the case of infinite U, a NDC is observed around $2(\lambda_\beta+U)$ even for a series CQD with weak interdot coupling $\Omega/\Gamma\leqslant 0.5$. This NDC behavior was first reported in our previous study[18] and was ascribed to decoherence effect in coherent tunneling due to the coupling to leads.[25,44] From Figs. 8(b) and 8(c), we observe that this NDC is robust against the additional pathway Γ' in the absence of magnetic flux and it is tuned to positive differential conductance when applying the magnetic field. It is worth noting that in the case of weak interdot Coulomb repulsion, above mentioned magnetic-flux-controlled NDC still remains around the boundary between configurations (f) and (c) [here, configuration (c) is at the bias voltage region $3<V<5$].

V. ZERO-FREQUENCY SHOT NOISE

A. Two-terminal number-resolved quantum rate equations and MacDonald's formula

This section is concerned with the discussion of zero-frequency current noise of the CQD interferometer in the case of $U\to\infty$. For this purpose, we employ MacDonald's formula for shot noise[47] based on a number-resolved version of the QREs describing the number of completed tunneling events.[48] This can be straightforwardly derived from the established QREs [Eqs. (7a)–(7e)]. We introduce the two-terminal number-resolved density matrices $\rho_{\chi\chi'}^{(n,m)}(t)$, representing the probability that the system is in the electronic state $|\chi\rangle$ (for $\chi=\chi'$) or in the quantum superposition state (for $\chi\neq\chi'$) at time t together with n (m) electrons occupying the left (right) lead due to tunneling events. Obviously, $\rho_{\chi\chi'}(t)=\Sigma_{n,m}\rho_{\chi\chi'}^{(n,m)}(t)$ and the resulting two-terminal number-resolved QREs for arbitrary bias voltage and interdot hopping are

$$\dot{\rho}_{00}^{(n,m)}=-\left[c_\theta^2(\Gamma_{11\alpha}^{+}+\Gamma_{22\beta}^{+})+s_\theta^2(\Gamma_{11\beta}^{+}+\Gamma_{22\alpha}^{+})+\frac{1}{2}\sin\theta(\Gamma_{12\alpha}^{+}+\Gamma_{21\alpha}^{+}-\Gamma_{12\beta}^{+}-\Gamma_{21\beta}^{+})\right]\rho_{00}^{(n,m)}$$
$$+\left[c_\theta^2\Gamma_{L11\alpha}^{-}+s_\theta^2\Gamma_{L22\alpha}^{-}+\frac{1}{2}\sin\theta(\Gamma_{L12\alpha}^{-}+\Gamma_{L21\alpha}^{-})\right]\rho_{\alpha\alpha}^{(n-1,m)}+\left[c_\theta^2\Gamma_{R11\alpha}^{-}+s_\theta^2\Gamma_{R22\alpha}^{-}+\frac{1}{2}\sin\theta(\Gamma_{R12\alpha}^{-}+\Gamma_{R21\alpha}^{-})\right]\rho_{\alpha\alpha}^{(n,m-1)}$$
$$+\left[s_\theta^2\Gamma_{L11\beta}^{-}+c_\theta^2\Gamma_{L22\beta}^{-}-\frac{1}{2}\sin\theta(\Gamma_{L12\beta}^{-}+\Gamma_{L21\beta}^{-})\right]\rho_{\beta\beta}^{(n-1,m)}+\left[s_\theta^2\Gamma_{R11\beta}^{-}+c_\theta^2\Gamma_{R22\beta}^{-}-\frac{1}{2}\sin\theta(\Gamma_{R12\beta}^{-}+\Gamma_{R21\beta}^{-})\right]\rho_{\beta\beta}^{(n,m-1)}$$

$$+\frac{1}{4}\sin\theta(\Gamma^-_{L11\alpha}+\Gamma^-_{L11\beta}-\Gamma^-_{L22\alpha}-\Gamma^-_{L22\beta})(\rho^{(n-1,m)}_{\alpha\beta}+\rho^{(n-1,m)}_{\beta\alpha})+\frac{1}{4}\sin\theta(\Gamma^-_{R11\alpha}+\Gamma^-_{R11\beta}-\Gamma^-_{R22\alpha}-\Gamma^-_{R22\beta})(\rho^{(n,m-1)}_{\alpha\beta}+\rho^{(n,m-1)}_{\beta\alpha})$$

$$+\frac{1}{2}[s^2_\theta(\Gamma^-_{L12\alpha}+\Gamma^-_{L12\beta})-c^2_\theta(\Gamma^-_{L21\alpha}+\Gamma^-_{L21\beta})]\rho^{(n-1,m)}_{\alpha\beta}+\frac{1}{2}[s^2_\theta(\Gamma^-_{R12\alpha}+\Gamma^-_{R12\beta})-c^2_\theta(\Gamma^-_{R21\alpha}+\Gamma^-_{R21\beta})]\rho^{(n,m-1)}_{\alpha\beta}$$

$$-\frac{1}{2}[c^2_\theta(\Gamma^-_{L12\alpha}+\Gamma^-_{L12\beta})-s^2_\theta(\Gamma^-_{L21\alpha}+\Gamma^-_{L21\beta})]\rho^{(n-1,m)}_{\beta\alpha}-\frac{1}{2}[c^2_\theta(\Gamma^-_{R12\alpha}+\Gamma^-_{R12\beta})-s^2_\theta(\Gamma^-_{R21\alpha}+\Gamma^-_{R21\beta})]\rho^{(n,m-1)}_{\beta\alpha}, \tag{23a}$$

$$\dot\rho^{(n,m)}_{\alpha\alpha}=\left[c^2_\theta\Gamma^+_{L11\alpha}+s^2_\theta\Gamma^+_{L22\alpha}+\frac{1}{2}\sin\theta(\Gamma^+_{L12\alpha}+\Gamma^+_{L21\alpha})\right]\rho^{(n+1,m)}_{00}+\left[c^2_\theta\Gamma^+_{R11\alpha}+s^2_\theta\Gamma^+_{R22\alpha}+\frac{1}{2}\sin\theta(\Gamma^+_{R12\alpha}+\Gamma^+_{R21\alpha})\right]\rho^{(n,m+1)}_{00}$$

$$-\left[c^2_\theta\Gamma^-_{11\alpha}+s^2_\theta\Gamma^-_{22\alpha}+\frac{1}{2}\sin\theta(\Gamma^-_{12\alpha}+\Gamma^-_{21\alpha})\right]\rho^{(n,m)}_{\alpha\alpha}-\frac{1}{4}\sin\theta(\Gamma^-_{11\beta}-\Gamma^-_{22\beta})(\rho^{(n,m)}_{\alpha\beta}+\rho^{(n,m)}_{\beta\alpha})$$

$$-\frac{1}{2}(s^2_\theta\Gamma^-_{12\beta}-c^2_\theta\Gamma^-_{21\beta})\rho^{(n,m)}_{\alpha\beta}-\frac{1}{2}(s^2_\theta\Gamma^-_{21\beta}-c^2_\theta\Gamma^-_{12\beta})\rho^{(n,m)}_{\beta\alpha}, \tag{23b}$$

$$\dot\rho^{(n,m)}_{\beta\beta}=\left[s^2_\theta\Gamma^+_{L11\beta}+c^2_\theta\Gamma^+_{L22\beta}-\frac{1}{2}\sin\theta(\Gamma^+_{L12\beta}+\Gamma^+_{L21\beta})\right]\rho^{(n+1,m)}_{00}+\left[s^2_\theta\Gamma^+_{R11\beta}+c^2_\theta\Gamma^+_{R22\beta}-\frac{1}{2}\sin\theta(\Gamma^+_{R12\beta}+\Gamma^+_{R21\beta})\right]\rho^{(n,m+1)}_{00}$$

$$-\left[s^2_\theta\Gamma^-_{11\beta}+c^2_\theta\Gamma^-_{22\beta}-\frac{1}{2}\sin\theta(\Gamma^-_{12\beta}+\Gamma^-_{21\beta})\right]\rho^{(n,m)}_{\beta\beta}-\frac{1}{4}\sin\theta(\Gamma^-_{11\alpha}-\Gamma^-_{22\alpha})(\rho^{(n,m)}_{\alpha\beta}+\rho^{(n,m)}_{\beta\alpha})$$

$$-\frac{1}{2}(s^2_\theta\Gamma^-_{12\alpha}-c^2_\theta\Gamma^-_{21\alpha})\rho^{(n,m)}_{\alpha\beta}-\frac{1}{2}(s^2_\theta\Gamma^-_{21\alpha}-c^2_\theta\Gamma^-_{12\alpha})\rho^{(n,m)}_{\beta\alpha}, \tag{23c}$$

$$\dot\rho^{(n,m)}_{\alpha\beta}=i2\Delta\rho^{(n,m)}_{\alpha\beta}+\left[\frac{1}{4}\sin\theta(\Gamma^+_{L11\alpha}+\Gamma^+_{L11\beta}-\Gamma^+_{L22\alpha}-\Gamma^+_{L22\beta})-\frac{1}{2}c^2_\theta(\Gamma^+_{L12\alpha}+\Gamma^+_{L12\beta})+\frac{1}{2}s^2_\theta(\Gamma^+_{L21\alpha}+\Gamma^+_{L21\beta})\right]\rho^{(n+1,m)}_{00}$$

$$+\left[\frac{1}{4}\sin\theta(\Gamma^+_{R11\alpha}+\Gamma^+_{R11\beta}-\Gamma^+_{R22\alpha}-\Gamma^+_{R22\beta})-\frac{1}{2}c^2_\theta(\Gamma^+_{R12\alpha}+\Gamma^+_{R12\beta})+\frac{1}{2}s^2_\theta(\Gamma^+_{R21\alpha}+\Gamma^+_{R21\beta})\right]\rho^{(n,m+1)}_{00}$$

$$-\frac{1}{2}\left[c^2_\theta(\Gamma^-_{11\alpha}+\Gamma^-_{22\beta})+s^2_\theta(\Gamma^-_{11\beta}+\Gamma^-_{22\alpha})-\frac{1}{2}\sin\theta(\Gamma^+_{12\alpha}+\Gamma^+_{21\alpha}-\Gamma^+_{12\beta}-\Gamma^+_{21\beta})\right]\rho^{(n,m)}_{\alpha\beta}$$

$$+\frac{1}{2}\left[c^2_\theta\Gamma^-_{12\alpha}-s^2_\theta\Gamma^-_{21\alpha}-\frac{1}{2}\sin\theta(\Gamma^-_{11\alpha}-\Gamma^-_{22\alpha})\right]\rho^{(n,m)}_{\alpha\alpha}+\frac{1}{2}\left[c^2_\theta\Gamma^-_{12\beta}-s^2_\theta\Gamma^-_{21\beta}-\frac{1}{2}\sin\theta(\Gamma^-_{11\beta}-\Gamma^-_{22\beta})\right]\rho^{(n,m)}_{\beta\beta}. \tag{23d}$$

The current of lead η can be evaluated as

$$I_\eta=\dot N_\eta(t)=\frac{d}{dt}\sum_{n,m}n_\eta P^{(n,m)}(t)\Big|_{t\to\infty}, \tag{24}$$

where

$$P^{(n,m)}(t)=\rho^{(n,m)}_{00}(t)+\rho^{(n,m)}_{11}(t)+\rho^{(n,m)}_{22}(t) \tag{25}$$

is the total probability of transferring n (m) electrons into the left (right) lead by time t and $n_\eta=n$ (m) if $\eta=L$ (R). It is easily verified that the current obtained from Eq. (24) by means of the number-resolved QREs [Eqs. (23a)–(23d)] is exactly the same as that obtained from Eq. (12). The zero-frequency shot noise with respect to lead η is similarly defined in terms of $P^{(n,m)}(t)$ as well:[22,29,47,48]

$$S_\eta(0)=2\frac{d}{dt}\left[\sum_{n,m}n^2_\eta P^{(n,m)}(t)-(tI_\eta)^2\right]\Big|_{t\to\infty}. \tag{26}$$

To evaluate $S_\eta(0)$, we define an auxiliary function $G^\eta_{\chi\chi'}(t)$ as

$$G^\eta_{\chi\chi'}(t)=\sum_{n,m}n_\eta\rho^{(n,m)}_{\chi\chi'}(t), \tag{27}$$

whose equations of motion can be readily deduced employing the number-resolved QREs [Eqs. (23a)–(23d)] in matrix form: $\dot{\boldsymbol{G}}^\eta(t)=\mathcal{M}_\eta\boldsymbol{G}^\eta(t)+\mathcal{G}_\eta\boldsymbol{\rho}(t)$, with $\boldsymbol{G}^\eta(t)=(G^\eta_{00},G^\eta_{\alpha\alpha},G^\eta_{\beta\beta},G^\eta_{\alpha\beta},G^\eta_{\beta\alpha})^T$ and $\boldsymbol{\rho}(t)=(\rho_{00},\rho_{\alpha\alpha},\rho_{\beta\beta},\rho_{\alpha\beta},\rho_{\beta\alpha})^T$. $\mathcal{M}_\eta$ and $\mathcal{G}_\eta$ can be read easily from Eqs. (23a)–(23d). Applying the Laplace transform to these equations yields

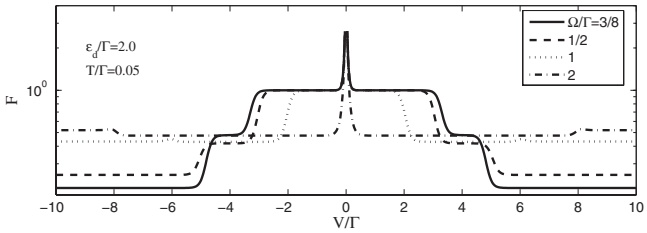

FIG. 9. Calculated Fano factor, $F=S(0)/2I$, for the series-connected CQD with $\varepsilon_d/\Gamma=2.0$ and various values of Ω/Γ (3/8, 1/2, 1, and 2). The temperature is $T/\Gamma=0.05$.

$$\boldsymbol{G}^{\eta}(s) = (s\boldsymbol{I} - \mathcal{M}_{\eta})^{-1}\mathcal{G}_{\eta}\boldsymbol{\rho}(s), \tag{28}$$

where $\boldsymbol{\rho}(s)$ is readily obtained by applying the Laplace transform to its equations of motion with the initial condition $\boldsymbol{\rho}(0)=\boldsymbol{\rho}_{st}$ [$\boldsymbol{\rho}_{st}$ denotes the stationary solution of the QREs, Eqs. (7a)–(7e)]. Due to the inherent long-time stability of the physical system under consideration, all real parts of nonzero poles of $\boldsymbol{\rho}(s)$ and $\boldsymbol{G}^{\eta}(s)$ are negative definite. Consequently, the divergent terms arising in the partial fraction expansions of $\boldsymbol{\rho}(s)$ and $\boldsymbol{G}^{\eta}(s)$ as $s\to 0$ entirely determine the large-t behavior of the auxiliary functions, i.e., the zero-frequency shot noise [Eq. (26)].

It is worth mentioning that (1) our two-terminal number-resolved QREs [Eqs. (23a)–(23d)] facilitate evaluation of the bias-voltage-dependent zero-frequency shot noise for arbitrary interdot hopping, and (2) our calculations yield $S_L(0)=S_R(0)$.

B. Results and discussion

We confined our studies to the case $\varepsilon_d>0$. The Fano factor, $F=S(0)/2I$, is used as the main tool to classify current.[19] It should be noted that because we use the formula $F=S(0)/2I$ to calculate it numerically, the Fano factor shown in the figures below is physically meaningful only when current increases above zero to avoid numerical divergence. Thus, our calculated Fano factor is physically meaningful only for configurations (f) and (c).

To start, we discuss shot noise for a series-connected CQD with symmetric geometry, $\Gamma_{L11}=\Gamma_{R22}=\Gamma$. In the case of configuration (c), i.e., the extremely large bias-voltage limit with zero temperature, we obtain an analytical expression for the Fano factor:[29]

$$F_c = \frac{80x^4 - 8x^2 + 1}{(1+12x^2)^2}, \tag{29}$$

with $x=\Omega/\Gamma$. For configuration (f), i.e., with appropriately small bias voltage, we have

$$F_f = \frac{8192x^4 + 896x^2 + 441}{(21+128x^2)^2}. \tag{30}$$

The results indicate sub-Poissonian shot noise, i.e., $F<1$, in the effective bias-voltage regime for any dot-dot hopping strength, as shown in Fig. 9. If the dot-dot hopping strength is set moderately weak, $\Omega/\Gamma\leqslant 0.978$ (which can be achieved by tuning the coupling potential between the two dots via applied gate voltage), we have $F_f>F_c$; otherwise, $F_f<F_c$.

We also examine the effect of the bias-voltage-induced shifting of bare levels on the shot noise in Fig. 10. It is shown that this shifting results in (i) a weak enhancement of the shot noise, i.e., a super-Poissonian noise to be a companion to the NDC when the eigenlevel β dominates in transport, and (ii) a constant Fano factor $F=1/2$ at the extremely large bias-voltage region.

Focusing attention on the more general parallel CQD geometry, we discuss the quantum interference effect of the additional pathway on shot noise. Our calculated results in the absence of magnetic flux are plotted in Fig. 11, including the shot noise $S(0)$ (normalized to $\frac{e^2}{\hbar}\Gamma$), the current I (normalized to $\frac{e}{\hbar}\Gamma$) for comparison, and the Fano factor. We find that the system exhibits a huge Fano factor with increasing tunneling rate of the additional branch in the case of configuration (c).[29] At zero temperature, we arrive at analytical expressions

$$I_c = \frac{4x^2\Gamma(\gamma+1)}{(\gamma+1)^2+12x^2}, \tag{31}$$

$$\begin{aligned} F_c = {} & [(80\gamma^2+352\gamma+80)x^4 + (-8\gamma^4+160\gamma^3+336\gamma^2+160\gamma \\ & -8)x^2 + \gamma^6+10\gamma^5+31\gamma^4+44\gamma^3+31\gamma^2+10\gamma+1] \\ & \times(\gamma-1)^{-2}[(\gamma+1)^2+12x^2]^{-2}, \end{aligned} \tag{32}$$

with $x=\Omega/\Gamma$ and $\gamma=\Gamma'/\Gamma$. It is obvious that (1) in the case of a series CQD, Eq. (32) reduces exactly to Eq. (29), exhibiting sub-Poissonian behavior; and in contrast, (2) $F_c>1$ with increasing γ.[29]

It should be noted that all calculations in the present paper are performed under the assumption of full interference between the two pathways and infinite interdot Coulomb repulsion. If decoherence is taken into account due to some dissipative mechanisms, the degree of interference will naturally lessen, thus leading to a great suppression of the Fano factor. In particular, in the case of full noninterference, the Fano factor reduces to a constant $F=10/27$, exhibiting sub-

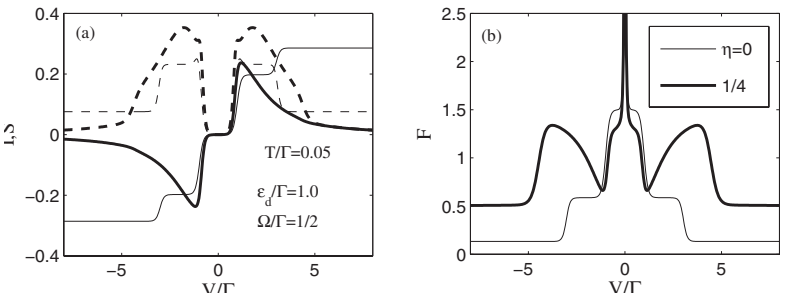

FIG. 10. (a) Zero-frequency shot noise $S(0)$ (dashed lines) and tunneling current I (solid lines), and (b) the Fano factor F, for the series CQD with $\varepsilon_d/\Gamma=1.0$, $\Omega/\Gamma=1/2$, and shifting factors $\eta=0$ and 1/4. The temperature is $T/\Gamma=0.05$.

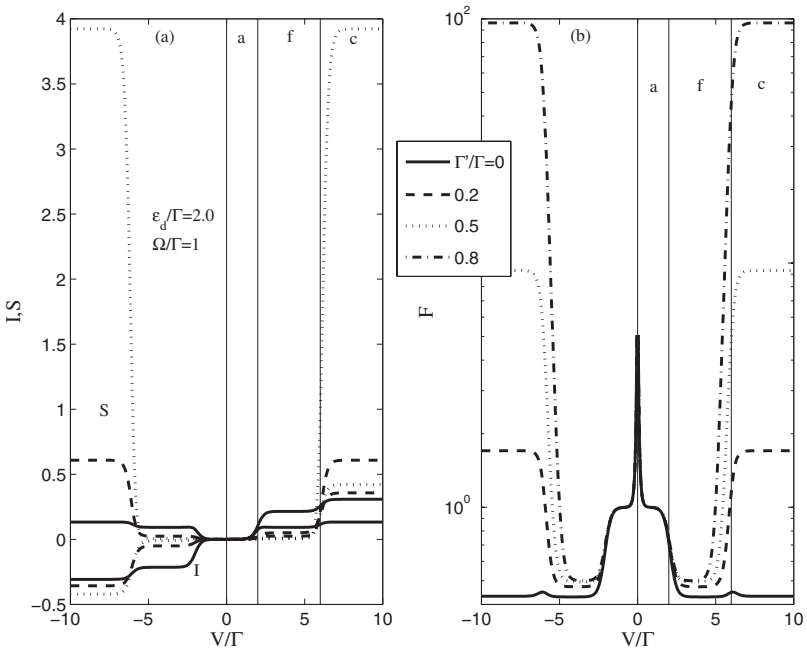

FIG. 11. (a) Zero-frequency shot noise $S(0)$ and tunneling current I, and (b) the Fano factor F, for the case $\varepsilon_d/\Gamma=2.0$ and $\Omega/\Gamma=1$ with various values of Γ'/Γ in the absence of magnetic flux. The temperature is $T/\Gamma=0.1$.

Poissonian shot noise. On the other hand, it has been reported that the noise is always sub-Poissonian in the case of no interdot Coulomb interaction.[29]

The phase effect on shot noise in a CQD interferometer tuned by magnetic flux is of special interest for configurations (c) and (f). We exhibit the magnetic-flux dependence of current, shot noise, and Fano factor in Fig. 12 with $\Gamma'/\Gamma=0.5$ at zero temperature. Due to interdot hopping, both the current and shot noise exhibit periodic oscillations with period 4π (as well as the Fano factor) for configuration (f). The current nearly vanishes around zero magnetic flux, $\varphi=0$, as indicated in Fig. 6(b) in Sec. IV C, while the shot noise is suppressed more strongly due to the effect of perfectly destructive quantum interference. In contrast, constructive

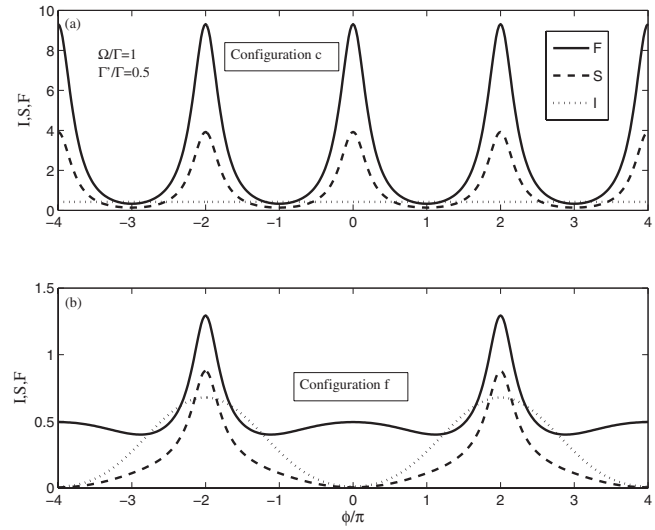

FIG. 12. Calculated magnetic-flux dependence of the zero-frequency shot noise $S(0)$, tunneling current I, and the Fano factor $F=S(0)/2I$ for a system with $\Omega/\Gamma=1.0$ and $\Gamma'/\Gamma=0.5$ in configuration (c) [panel (a)] and (f) [panel (b)] at zero temperature.

quantum interference enhances the zero-frequency shot noise more than the current, giving rise to super-Poissonian noise $F\simeq 5/4$ at $\varphi=\pm 2\pi$ even for configuration (f). On the other hand, the shot noise for configuration (c) displays a different magnetic-flux dependence from that of configuration (f). Both $S(0)$ and F are observed to behave as $\sim|\sin(\varphi)|$. Interestingly, varying magnetic flux could change the shot noise from super-Poissonian, $F\simeq 10$ at $\varphi=2n\pi$ (n is an integer), to sub-Poissonian, $F\simeq 0.33$ at $\varphi=2(n+1)\pi$. Actually, we have derived an analytical expression for noise in configuration (c) and $\varphi=\pm\pi$:

$$F_c=[80x^4-8(\gamma^2+2\gamma+1)x^2+\gamma^4+4\gamma^3+6\gamma^2+4\gamma+1]\times[(\gamma+1)^2+12x^2]^{-2}, \quad (33)$$

indicating sub-Poissonian noise. It is also of interest to point out that at these values of magnetic flux [φ around $2(n+1)\pi$], the quantum interference effect induces NDC even for a very weak tunneling rate of the additional pathway, $\Gamma'/\Gamma=0.1$, as indicated in Figs. 6 and 7 in Sec. IV C (roughly $\varphi\geqslant 1.2\pi$), but super-Poissonian noise is not necessarily an accompaniment of this magnetic-flux-tuned NDC.

VI. CONCLUSIONS

In summary, we have analyzed first-order transport through a CQD AB interferometer with finite dot-dot hopping, determining the I-V characteristics, zero-frequency current noise, and their magnetic-flux dependence. To accomplish this, we established generic QREs in terms of the ER, employing a quantum Langevin equation approach in the weak-tunneling limit. These QREs are valid for arbitrary temperature and bias voltage, as well as arbitrary dot-dot hopping, improving upon our previous derivation which was limited by the restriction that interdot hopping be much weaker than dot-lead coupling, i.e., $\Omega\ll\Gamma$.

We have also derived the current and Schottky-type shot noise formulas in terms of the RDM elements. Our theory

proves that the previous scheme for evaluating the frequency-independent part of the classical intrinsic shot noise (i.e., all tunneling processes providing contributions to current always yield positive contributions to the Schottky-type shot noise) remains valid in the formulation of quantum-based rate equations in the ER.

Employing the QREs derived here, we have systematically analyzed coherent resonant tunneling through a CQD in series and parallel configurations, respectively. By discussing the variation of the energetic configuration with increasing bias voltage, we have explained the asymmetric transport property in the series CQD. We have also examined the effect of the bias-voltage-induced shifting of bare levels of the CQD and found the appearance of a NDC. For the parallel CQD, our numerical results have shown that (1) the current of configuration (c) is independent of magnetic flux due to the combination of full interference and strong Coulomb blockade effect; (2) AB oscillations emerge in the current in the small bias-voltage regime, i.e., the case of configuration (f); and (3) the current nearly vanishes completely around $\varphi=0$ due to perfect destructive interference, while it is greatly enhanced around $\varphi=2\pi$ due to constructive interference, and it may even be much larger than the current of configuration (c), suggesting the possibility of magnetic-flux-controllable NDC.

Finally, we have investigated zero-frequency shot noise using MacDonald's formula by rewriting the fully developed QREs in terms of a two-terminal number-resolved density-matrix form. The main result we obtained is that the combined effect of interference between two path branches and the infinite interdot Coulomb interaction may induce a huge Fano factor, which can also be controlled by manipulating magnetic flux.

ACKNOWLEDGMENTS

This work was supported by Projects of the National Science Foundation of China, the Shanghai Municipal Commission of Science and Technology, the Shanghai Pujiang Program, and Program for New Century Excellent Talents in University (NCET). N.J.M.H. was supported by the DURINT program administered by the U.S. Army Research Office, DAAD Grant No. 19-01-1-0592.

[1] H. Haug and A.-P. Jauho, *Quantum Kinetics in Transport and Optics of Semiconductors* (Springer, Berlin, 1996).
[2] W. G. van der Wiel, S. De Franceschi, J. M. Elzerman, T. Fujisawa, S. Tarucha, and L. P. Kouwenhoven, Rev. Mod. Phys. **75**, 1 (2003).
[3] A. W. Holleitner, C. R. Decker, H. Qin, K. Eberl, and R. H. Blick, Phys. Rev. Lett. **87**, 256802 (2001).
[4] A. W. Holleitner, R. H. Blick, A. K. Hüttel, K. Eberl, and J. P. Kotthaus, Science **297**, 70 (2002).
[5] J. C. Chen, A. M. Chang, and M. R. Melloch, Phys. Rev. Lett. **92**, 176801 (2004).
[6] D. Loss and E. V. Sukhorukov, Phys. Rev. Lett. **84**, 1035 (2000).
[7] E. V. Sukhorukov, G. Burkard, and D. Loss, Phys. Rev. B **63**, 125315 (2001).
[8] Lev G. Mourokh, N. J. M. Horing, and A. Yu. Smirnov, Phys. Rev. B **66**, 085332 (2002).
[9] J. König and Y. Gefen, Phys. Rev. B **65**, 045316 (2002).
[10] B. Kubala and J. König, Phys. Rev. B **65**, 245301 (2002).
[11] T. V. Shahbazyan and M. E. Raikh, Phys. Rev. B **49**, 17123 (1994).
[12] M. L. Ladrón de Guevara, F. Claro, and P. A. Orellana, Phys. Rev. B **67**, 195335 (2003).
[13] Bing Dong, Ivana Djuric, H. L. Cui, and X. L. Lei, J. Phys.: Condens. Matter **16**, 4303 (2004).
[14] Yu. V. Nazarov, Physica B **189**, 57 (1993).
[15] T. H. Stoof and Yu. V. Nazarov, Phys. Rev. B **53**, 1050 (1996); B. L. Hazelzet, M. R. Wegewijs, T. H. Stoof, and Yu. V. Nazarov, *ibid.* **63**, 165313 (2001).
[16] S. A. Gurvitz and Ya. S. Prager, Phys. Rev. B **53**, 15932 (1996).
[17] S. A. Gurvitz, Phys. Rev. B **57**, 6602 (1998).
[18] Bing Dong, H. L. Cui, and X. L. Lei, Phys. Rev. B **69**, 035324 (2004).
[19] Ya. M. Blanter and M. Büttiker, Phys. Rep. **336**, 1 (2000).
[20] C. Beenakker and C. Schönenberger, Phys. Today **56** (5), 37 (2003).
[21] H. B. Sun and G. J. Milburn, Phys. Rev. B **59**, 10748 (1999).
[22] B. Elattari and S. A. Gurvitz, Phys. Lett. A **292**, 289 (2002).
[23] R. Aguado and T. Brandes, Phys. Rev. Lett. **92**, 206601 (2004).
[24] I. Djuric, Bing Dong, and H. L. Cui, IEEE Trans. Nanotechnol. **4**, 71 (2005); Appl. Phys. Lett. **87**, 032105 (2005).
[25] I. Djuric, Bing Dong, and H. L. Cui, J. Appl. Phys. **99**, 063710 (2006).
[26] G. Kießlich, P. Samuelsson, A. Wacker, and E. Schöll, Phys. Rev. B **73**, 033312 (2006).
[27] G. Kießlich, A. Wacker, and E. Schöll, Phys. Rev. B **68**, 125320 (2003).
[28] J. Aghassi, A. Thielmann, M. H. Hettler, and G. Schön, Phys. Rev. B **73**, 195323 (2006).
[29] Bing Dong and X. L. Lei, arXiv:cond-mat/0611552 (unpublished).
[30] J. Schwinger, J. Math. Phys. **2**, 407 (1961).
[31] J. R. Ackerhalt and J. H. Eberly, Phys. Rev. D **10**, 3350 (1974).
[32] C. Cohen-Tannoudji, J. Dupont-Roc, and G. Grynberg, *Atom–Photon Interactions: Basic Processes and Applications* (Wiley, New York, 1992), pp. 334 and 388.
[33] P. W. Milonni, *The Quantum Vacuum: An Introduction to Quantum Electrodynamics* (Academic, San Diego, 1994).
[34] C. W. Gardiner and P. Zoller, *Quantum Noise* (Springer, Berlin, 1999).
[35] G. F. Efremov and A. Yu. Smirnov, Zh. Eksp. Teor. Fiz. **80**, 1071 (1981) [Sov. Phys. JETP **53**, 547 (1981)].
[36] Bing Dong, N. J. M. Horing, and H. L. Cui, Phys. Rev. B **72**, 165326 (2005).
[37] A. N. Korotkov, D. V. Averin, and K. K. Likharev, Phys. Rev. B **49**, 7548 (1994).
[38] G. D. Mahan, *Many-Particle Physics*, 3rd ed. (Kluwer Academic,

Dordrecht/Plenum, New York, 2000).
[39] J. H. Davies, P. Hyldgaard, S. Hershfield, and J. W. Wilkins, Phys. Rev. B **46**, 9620 (1992).
[40] A. N. Korotkov, D. V. Averin, K. K. Likharev, and S. A. Vasenko, in *Single-Electron Tunneling and Mesoscopic Devices*, edited by H. Koch and H. Lübbig, Springer Series in Electronics and Photonics Vol. 31 (Springer-Verlag, Berlin, 1992), p. 45; A. N. Korotkov, Phys. Rev. B **49**, 10381 (1994).
[41] H. M. Wiseman and G. J. Milburn, Phys. Rev. A **47**, 1652 (1993).
[42] S. Datta, W. Tian, S. Hong, R. Reifenberger, J. I. Henderson, and C. P. Kubiak, Phys. Rev. Lett. **79**, 2530 (1997); V. Mujica, A. E. Roitberg, and M. A. Ratner, J. Chem. Phys. **112**, 6834 (2000); S. Pleutin, H. Grabert, G. L. Ingold, and A. Nitzan, *ibid.* **118**, 3756 (2003).
[43] S. Lakshmi and S. K. Pati, Phys. Rev. B **72**, 193410 (2005); B. Song, D. A. Ryndyk, and G. Cuniberti, *ibid.* **76**, 045408 (2007).
[44] J. N. Pedersen, B. Lassen, A. Wacker, and M. H. Hettler, Phys. Rev. B **75**, 235314 (2007).
[45] J. Chen, M. A. Reed, A. M. Rawlett, and J. M. Tour, Science **286**, 1550 (2001).
[46] J. Ma, Bing Dong, and X. L. Lei, Eur. Phys. J. B **36**, 599 (2003).
[47] D. K. C. MacDonald, Rep. Prog. Phys. **12**, 56 (1948).
[48] L. Y. Chen and C. S. Ting, Phys. Rev. B **46**, 4714 (1992).